

## **Delineation of thin conglomerate deposits using multicomponent seismic data**

**Brad D. Nazar and Don C. Lawton**

### **ABSTRACT**

This study involved the analysis of a multicomponent data set acquired in the Carrot Creek oilfield of west-central Alberta. One of the unique features of this data is the presence of a strong radial-component (P-SV) amplitude anomaly at the location of oil-producing conglomerate deposits. The vertical (P-P) component, comparatively, exhibits only a subtle amplitude variation at the same location.

The Cardium conglomerate in this area was found to have a P-wave velocity of 4327 m/s and a Poisson's Ratio between 0.18 and 0.22. Over- and underlying the conglomerate are thick shale deposits having P-wave velocities of 3920 and 4003 m/s respectively, and a Poisson's Ratio of 0.31.

AVO forward modeling, shows a polarity reversal with offset occurring on the vertical (P-P) but not the radial component, for the conglomerate event. It is this polarity reversal on the vertical component which causes the poor amplitude response at the location of the Cardium conglomerate. Upon stacking, the near- and far-offsets of the vertical component add destructively whereas the radial-component offsets add constructively, thus causing the Cardium conglomerate to be more easily seen on the radial component section.

The P-P and P-SV data were found to be most sensitive to variation in conglomerate thickness over the 0-1000 m and 500-2000 m offset-ranges, respectively. From this result it was found that better imaging of the Cardium conglomerate could be achieved by either limiting the offset-range during acquisition or by generating offset-range stacks.

It was also found that by using both the P-P and P-SV data, estimates for Poisson's Ratio for specific seismic intervals could also be calculated. This interval analysis was in turn capable of identifying variations in conglomerate thickness by the presence of lows in the calculated Poisson's Ratios. Two such lows could be identified using the multicomponent data, which in turn correlate well with the location of the conglomerate deposits.

### **OBJECTIVES**

The objective of this study was to undertake the interpretation of a multicomponent seismic data set acquired in the Carrot Creek oilfield of west central Alberta. The specific items that were addressed in this study are as follows:

- 1) Explain differences in responses of the vertical and radial component of the multicomponent data set in terms of both lithology and formation thickness.

- 2) Study amplitude-versus-offset (AVO) effects on both the P-P and P-SV data.
- 3) Investigate if variations in lithology can be determined by coupling the P-P (vertical-component) and the P-SV (radial-component) data.
- 4) Study what source-receiver offsets are best for identifying the Cardium conglomerates of the Carrot Creek field.

In general, this study looks at the feasibility of using multicomponent data, acquired using conventional P-wave vibrators, as an exploration tool. The emphasis of this study being the effects of variation of thickness and lithology, of geologic units, on the P-P and P-SV seismic responses.

## GEOLOGY

### Study area

This study is located in the Carrot Creek area of west-central Alberta, approximately 150 km west of Edmonton (Figure 1). The study area encompasses townships 52-53, ranges 12-13 west of the fifth meridian, and is located just northwest of the Pembina oilfield. Figure 2 shows the well locations in the study area and the orientation of the multicomponent seismic lines. Initially discovered in 1963, the Carrot Creek field produces from primarily conglomerates, but also some sandstone units of the Cardium Formation. Present estimates of reserves for the field are placed at approximately 7 million barrels of initially recoverable oil and a further 2 million barrels of oil recoverable through waterflood (Bergman and Walker, 1987).

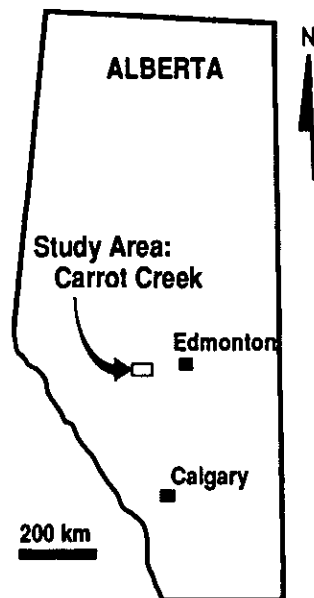


FIG. 1. Carrot Creek location map

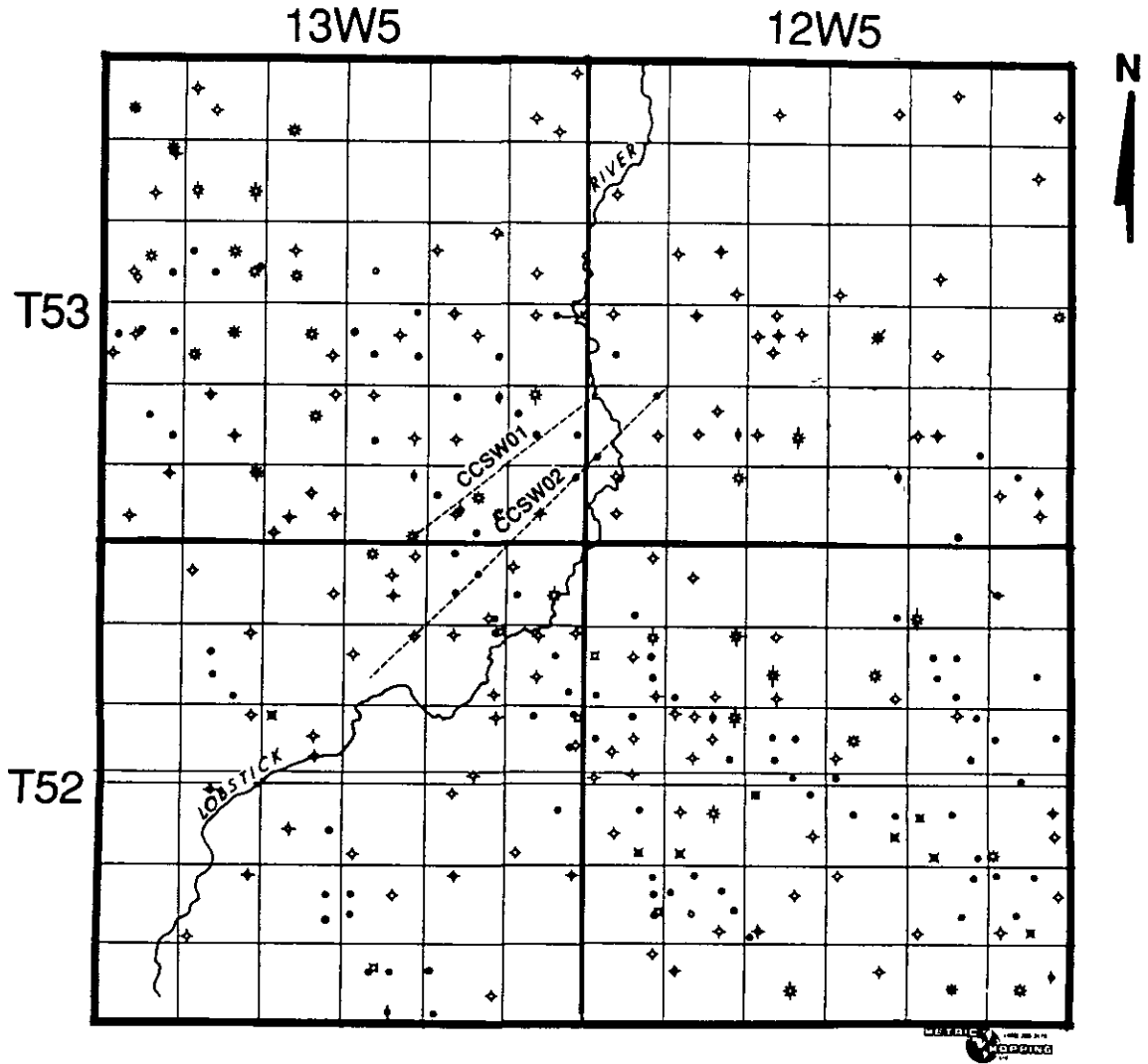


FIG. 2. Orientation of the Carrot Creek multicomponent seismic data

## Stratigraphy

Due to its location in the Central Plains of Alberta, the Carrot Creek field contains primarily flat-lying stratigraphy. The zone of interest for this field is the Upper Cretaceous Cardium Formation which contains oil reservoirs in stratigraphic traps. It produces from conglomerates and fine-grained sandstones that are believed to have been deposited in a shallow-marine environment.

The Cardium Formation in the Carrot Creek area occurs at a depth of approximately 1600 m below surface. It is both overlain and underlain by marine shales of the Wapiabi and Blackstone Formations respectively (Williams and Burk, 1964). Krause and Nelson (1984) recognized two distinct lithostratigraphic units within the Cardium Formation itself; the Cardium Zone Member and the Pembina River Member. Although this stratigraphy was based upon lithologies found in the Pembina field, it is consistent with those found in the Carrot Creek field (Krause and Nelson, 1984). The Cardium Zone Member, in the Carrot Creek field, consists primarily of marine shales with infrequent pebbly stringers (Krause and Nelson, 1984). The top of this member is marked by a chert pebble and nodular siderite layer.

The Pembina River Member underlies the Cardium Member and is made up of a coarsening-upward sequence of sediments (Krause and Nelson, 1984). It is variably thick throughout the Carrot Creek area reaching a maximum thickness of 30 m (Joiner, 1989). The sediments grade from silty mudstone at the base of the member through to sandstone and into, in some cases, thick conglomerates (Krause and Nelson, 1984). It is the presence of these thick conglomerates which distinguish the Carrot Creek field from the Pembina field. These conglomerates are found in bodies of up to 20 m thick (Plint et al. 1986) and are the primary reservoir rocks for the Carrot Creek field.

## GEOLOGIC MODEL

The geologic model used to represent the Carrot Creek field is shown in Figure 3. It is based upon well log and core data, and the following seismic interpretations. The model layers were horizontal, as this is a close approximation to the long wavelength geology of the area. The velocities, Poisson's Ratios, and densities for each layer are summarized in Table 1. Geologic markers, corresponding to seismic events identified on the seismic sections, were used to make up the model's layers. These markers were identified on the P-wave sections (conventional and vertical-component data) by correlating the surface seismic with synthetic seismograms generated from P-wave sonic logs found in the area (Figure 4). Figures 5 through 6 show the vertical-component migrated-stacks with and without the interpreted events.

Due to the lack of a complete full-waveform sonic or an offset VSP, events on the P-SV (radial-component) stacks were identified by visually correlating each radial-component stack with its respective vertical-component stack, as illustrated in Figure 7. To aid in the identification of events a P-wave synthetic along with a P-SV synthetic generated using the technique discussed by Howell et al (1991), are included. Figure 8 and 9 show the radial-component migrated stacks of both multicomponent lines with and without the interpreted events.

The P-wave velocity and density for each layer in the model (Table 1), were obtained

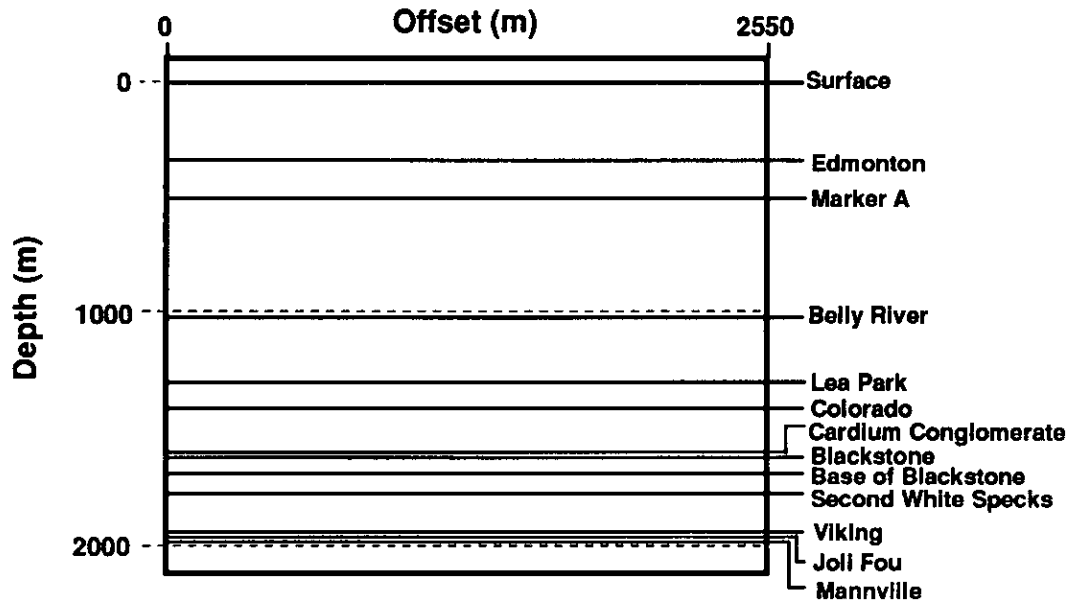


FIG. 3. Geometry of the Carrot Creek geologic model

Table 1 - Carrot Creek Model Parameters

Geologic Marker	Depth (m)	Thickness (m)	Vp (m/s)	Vs (m/s)	Vp/Vs	Poisson's Ratio	Density (gm/cm <sup>3</sup> )
Surface	0	355	2800	1040	2.58	0.42	2.37
Edmonton	355	200	3226	1198	2.58	0.42	2.37
Marker A	555	470	3200	1488	2.15	0.36	2.37
Belly River	1025	290	4150	2230	1.86	0.30	2.45
Lea Park	1315	117	3650	1889	1.93	0.31	2.50
Colorado	1432	178	3920	2057	1.93	0.31	2.38
Cardium (conglomerate)	1605-1620	5-20	4327	2591-2704	1.60-1.67	0.18-0.22	2.61
Blackstone	1625	80	4003	2100	1.91	0.31	2.51
Base of Blackstone	1690	85	3900	2267	1.73	0.25	2.55
Second White Specks	1775	150	3600	1999	1.80	0.28	2.45
Viking	1925	33	4400	2666	1.65	0.21	2.60
Joli Fou	1958	14	3800	2302	1.65	0.21	2.30
Mannville	1972	-	4200	2545	1.65	0.21	2.60

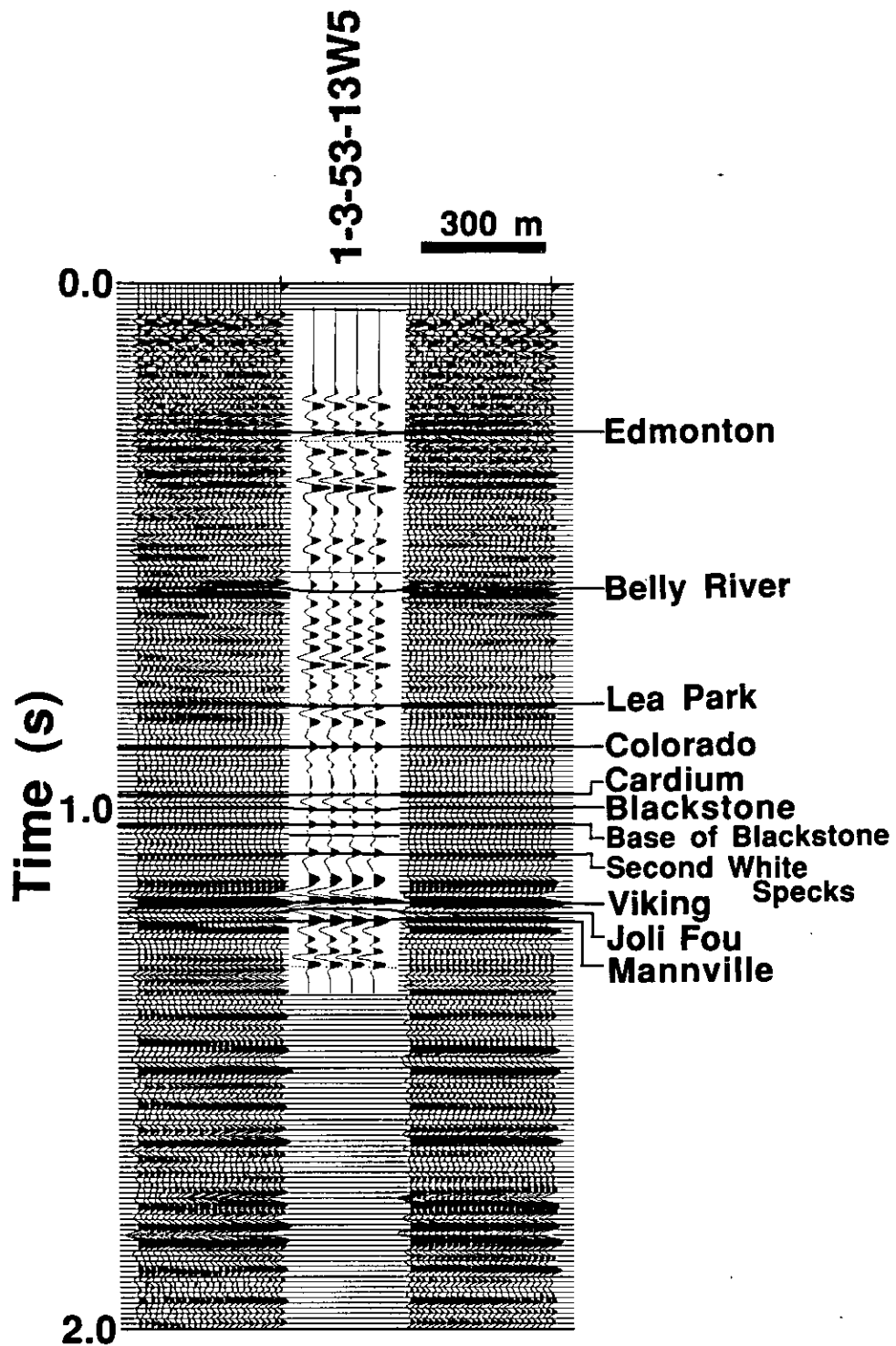


FIG. 4. Identification of events on the vertical component of line CCSW01 using a synthetic seismogram generated from the sonic log of well 1-3-53-13W5.

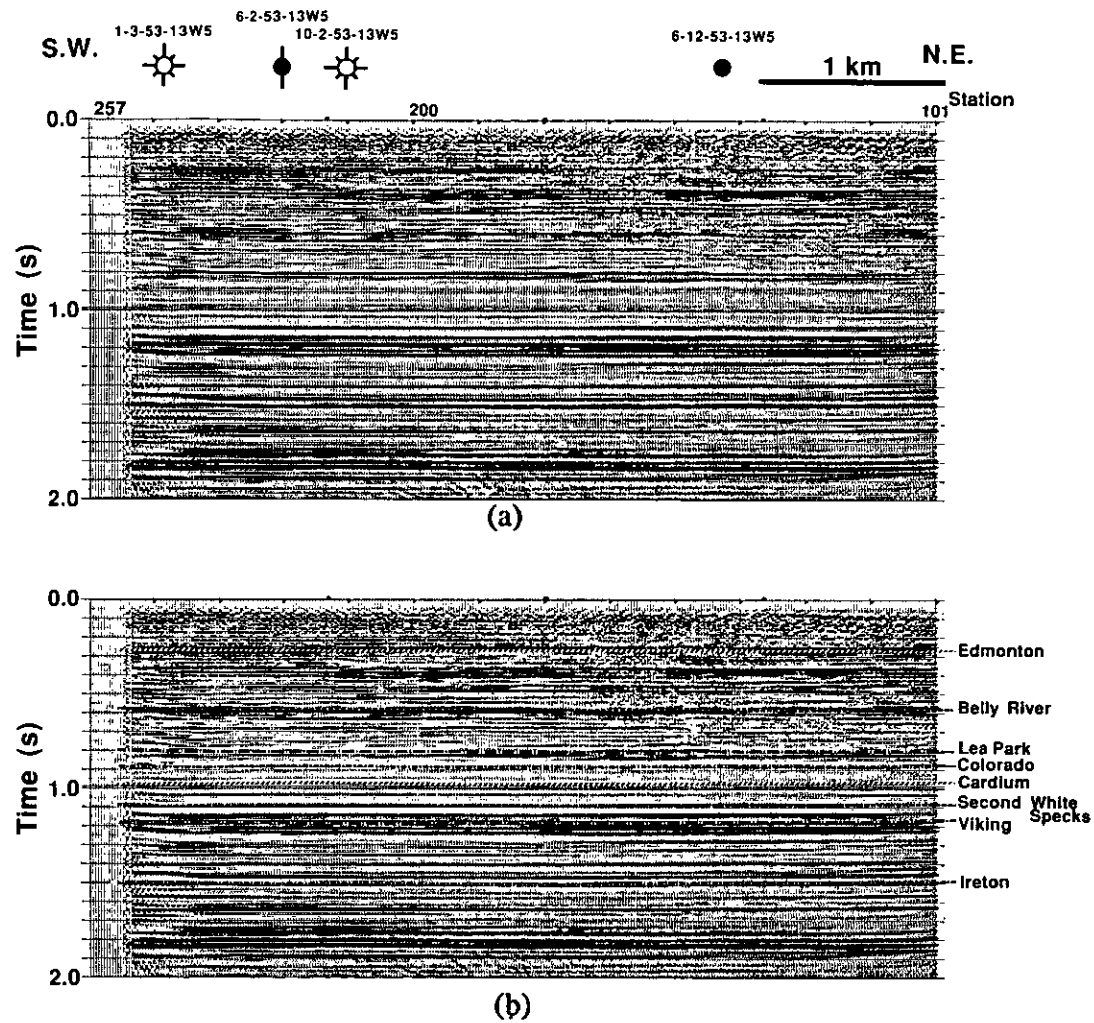


FIG. 5. Final migrated-stack of the vertical-component of line CCSW01 (a) without and (b) with interpreted events

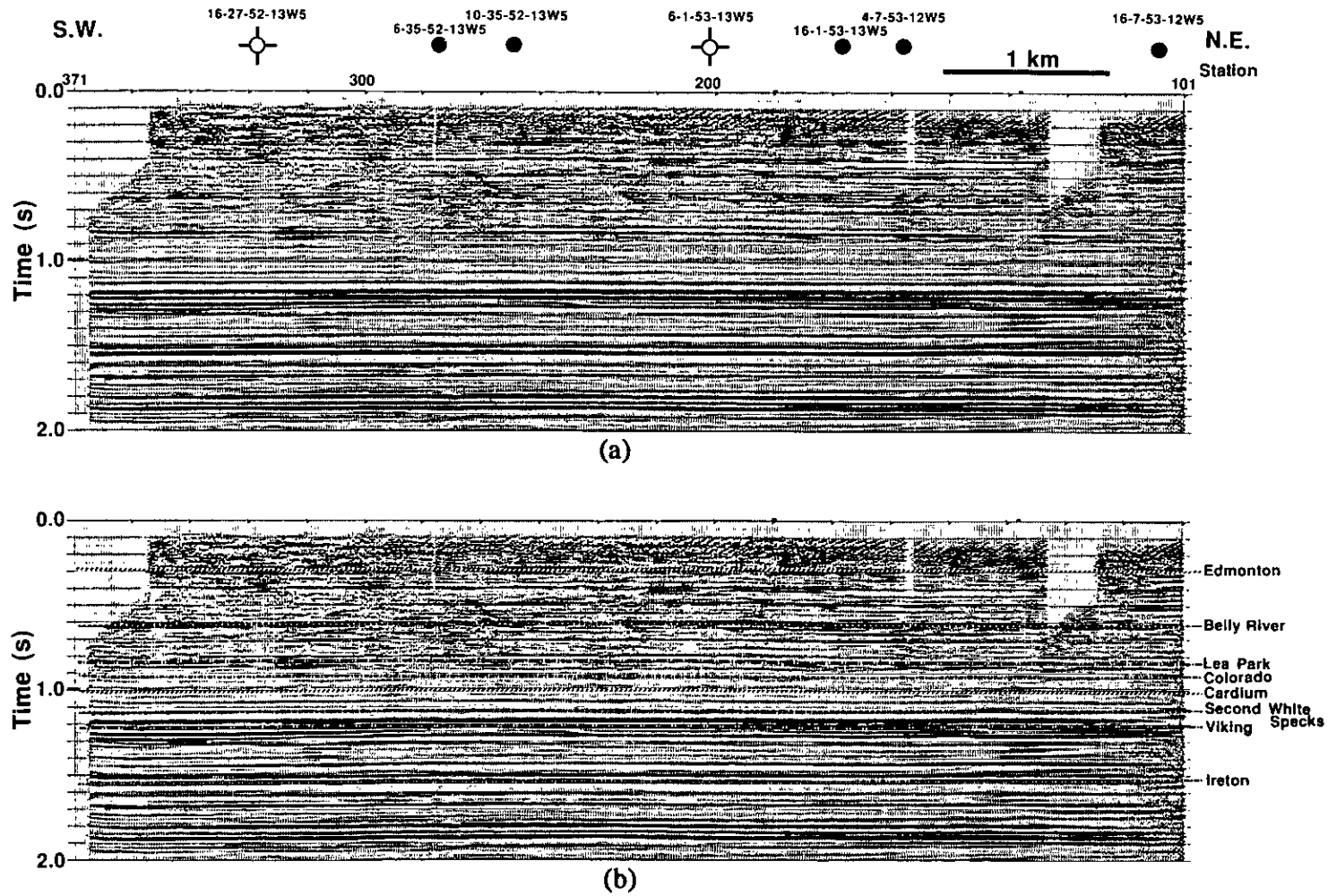


FIG. 6. Final migrated-stack of the vertical-component of line CCSW02 (a) without and (b) with interpreted events



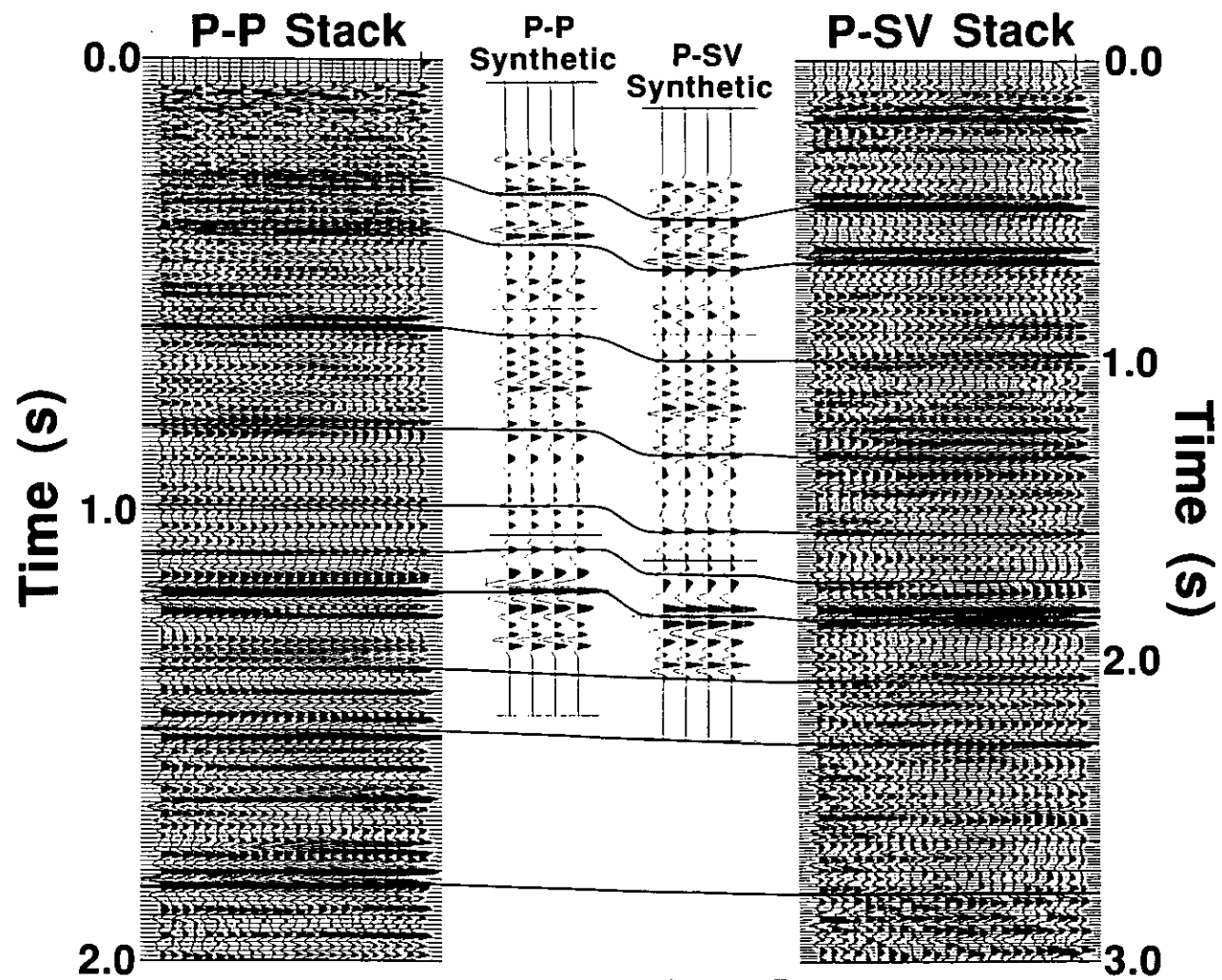


FIG. 7. Correlation between the vertical- and radial-components of line CCSW01, aided by P-P and P-SV synthetic seismograms from well 1-3-53-13W5.

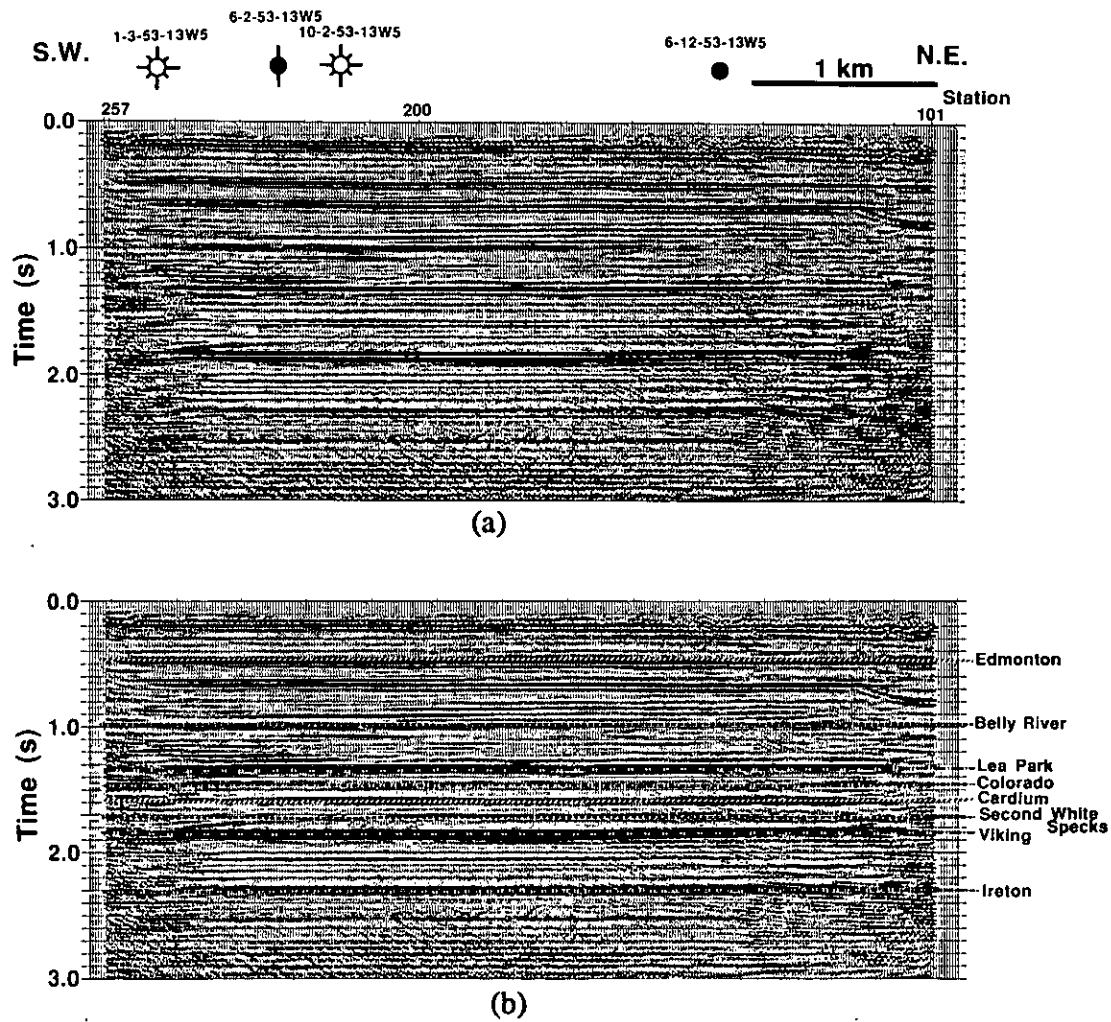


FIG. 8. Final migrated-stack of the radial-component of line CCSW01 (a) without and (b) with interpreted events

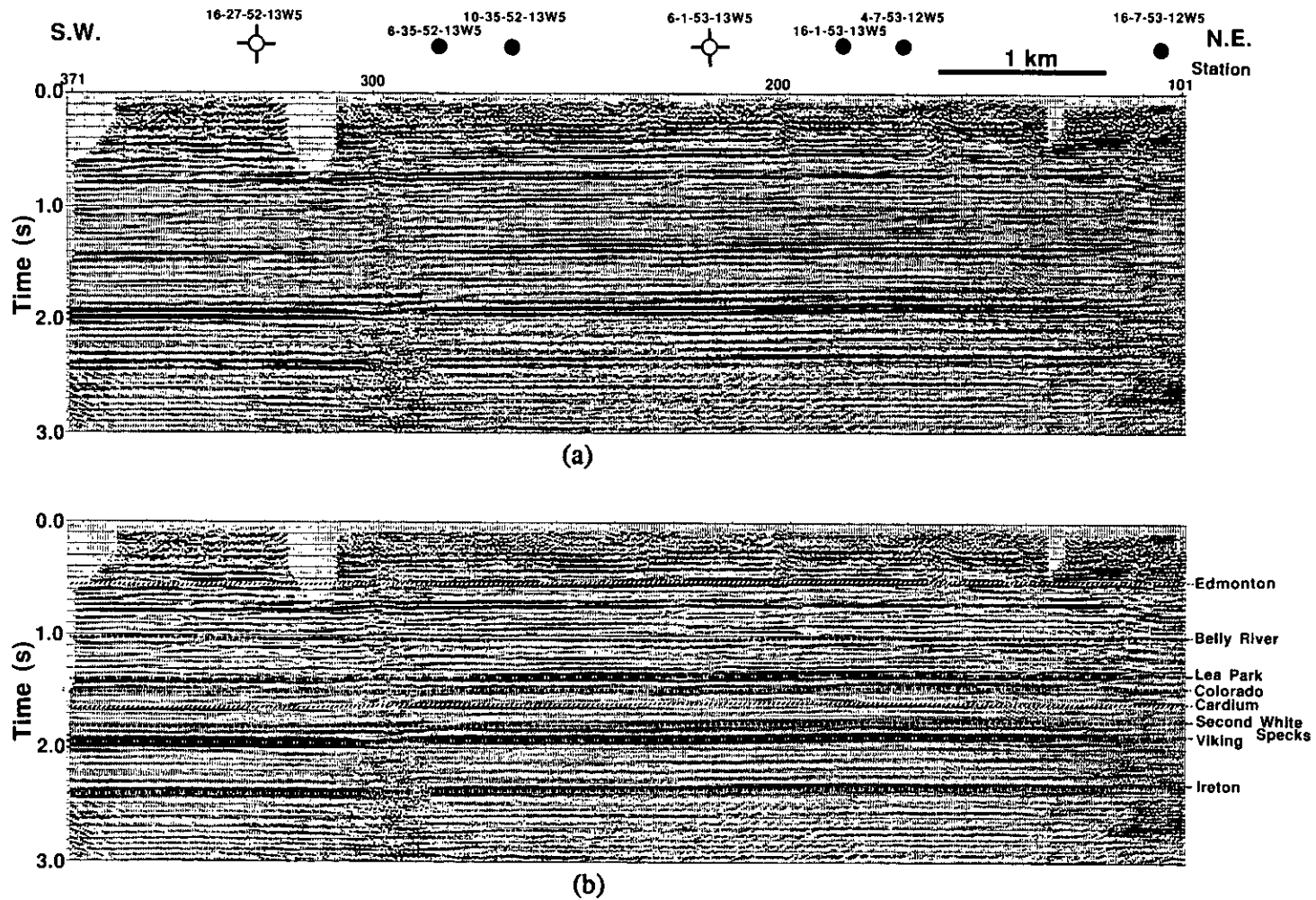


FIG. 9. Final migrated-stack of the radial-component of line CCSW02 (a) without and (b) with interpreted events

by blocking (ie. averaging) the sonic and density logs over the intervals defined by the geologic markers. Of the wells located in the study area, the sonic and density logs of well 1-3-53-13W5 were blocked. This well was chosen because it is located along seismic line CCSW01 and it is typical of wells in the area. The velocity ratios listed in Table 1, for the respective intervals were determined using the following equation;

$$\frac{V_p}{V_s} = \frac{2I_s}{I_p} - 1 \quad (\text{Harrison, 1989}), \quad (1)$$

where  $I_p$  and  $I_s$  are the time-intervals on the vertical- and radial-stacks respectively. Table 2 shows the results of these calculations. Using the interval  $V_p/V_s$  values and weighting them by their respective P-SV isochron, an average  $V_p/V_s$  down to each event was also calculated.

The seismic parameters of the Cardium conglomerate were based upon core analysis from well 6-12-53-13W5 and full-waveform sonic data collected over the Cardium Formation from wells 12-31-50-10W5 and 16-2-51-11W5, located just south-east of the study area. Using this data, the conglomerates of the Carrot Creek field were found to have an average velocity of 4327 m/s and a Poisson's Ratio between 0.18 and 0.22. These values are significantly different from those of the thick shale units of the Wabiabi and Blackstone Formations overlying and underlying the conglomerate. The velocities of these shales, determined from well 1-3-53-13W5, were found to be 3920 and 4003 m/s respectively. Using equation 1, the full-waveform sonic logs discussed previously and the following equation, the Poisson's Ratios of these shales were determined to be approximately 0.31.

$$\sigma = \frac{\frac{1}{2}\left(\frac{V_p}{V_s}\right)^2 - 1}{\left(\frac{V_p}{V_s}\right)^2 - 1} \quad (2)$$

**Table 2 - Compressional-to-shear velocities based upon interval times of the vertical (P-P) and radial (P-SV) data of line CCSW01**

Event Travel-time		Isochron		$V_p/V_s$	
P-P (ms)	P-SV (ms)	P-P (ms)	P-SV (ms)	Interval	Weighted
262	483	116	187	2.22	2.22
378	670	212	330	2.11	2.15
590	1000	224	320	1.86	2.03
816	1320	184	270	2.00	2.01
1000	1592	94	127	1.70	1.97
1094	1726	90	124	1.76	1.95
1185	1850	172	225	1.62	1.90
1356	2075	154	230	1.99	1.91
1510	2305	130	198	2.04	1.92
1640	2503	194	277	1.86	1.91
1834	2780				

## AVO MODELING

The significant difference in P-wave velocity and Poisson's Ratio of the Cardium conglomerate, with respect to the encompassing shales, produces an ideal situation to undertake amplitude-versus-offset (AVO) analysis. Both P-P (vertical-component) and P-SV (radial-component) AVO modeling was undertaken, using the velocities and densities listed in Table 1, to see if the conglomerate produces any observable AVO effects. Since the conglomerate deposits are isolated by thick over- and underlying shales, all modeling involved only the top and bottom interface of the conglomerate. The modeling was undertaken to a maximum source-receiver offset of 2550 m, which corresponds to the far-offset used during acquisition of the multicomponent seismic data. The P-P and P-SV AVO models were generated using Ricker wavelets of 30 and 20 Hz respectively. These frequencies were used since they were determined, using cross-power spectra, to be the dominant frequencies of the Cardium event in the final seismic sections.

Figure 10 and 11 show examples of plots of the P-P and P-SV amplitude and phase versus angle of incidence (determined using Zoeppritz equations) of reflections from the top and bottom interfaces of the conglomerate. In these examples, the overlying shale, conglomerate and the underlying shale were assumed to have P-wave velocities of 3920, 4327 and 4003 m/s (from Table 1), respectively. Poisson's Ratios, taken from Table 1, of 0.18 and 0.31 were assumed for the conglomerate and shales, respectively.

These figures show that both the P-P and P-SV reflection amplitudes and phases are highly dependent upon the angle of incidence. Several significant differences can be observed between their respective responses.

- 1) The P-P and P-SV amplitudes appear to be inversely related up to incident angles just less than the critical angle; P-P amplitudes are decreasing with increasing angle of incidence (e.g., from 0° to approximately 30°) whereas the P-SV amplitudes are increasing, and vice versa.
- 2) At small angles of incidence, for both a positive and negative impedance contrast (ie. top and bottom of the conglomerate), the P-P data will be phase-shifted 180° with respect to the P-SV data (ie. opposite polarity). This response results from the Aki and Richards' (1981) polarity convention.
- 3) At incident angle of approximately 38° and 29°, for the top and bottom interfaces respectively, the P-P amplitude decreases to zero. For incidence beyond these angles, the reflection amplitudes then increase but are 180° phase-shifted (ie. polarity reversed) to make the reflections the same phase as those for the P-SV data. Other phase shifts also occur past the critical angles, but these however will not be considered since incident angles this large are not reached in the Carrot Creek data set.

It should be noted that although these amplitude and phase plots represent the response for a specific set of velocities and densities, the trends observed would occur for any case in which the conglomerate has a higher P-wave velocity and lower Poisson's Ratio than the surrounding shale. Differences would only occur in relative amplitude and the position of the polarity changes.

### Tuning effect

The above results indicate that strong individual AVO effects should be produced from the top and bottom interfaces of the conglomerate. However, because of the thin nature of the conglomerate deposits, interference between the top and bottom events (ie. tuning of

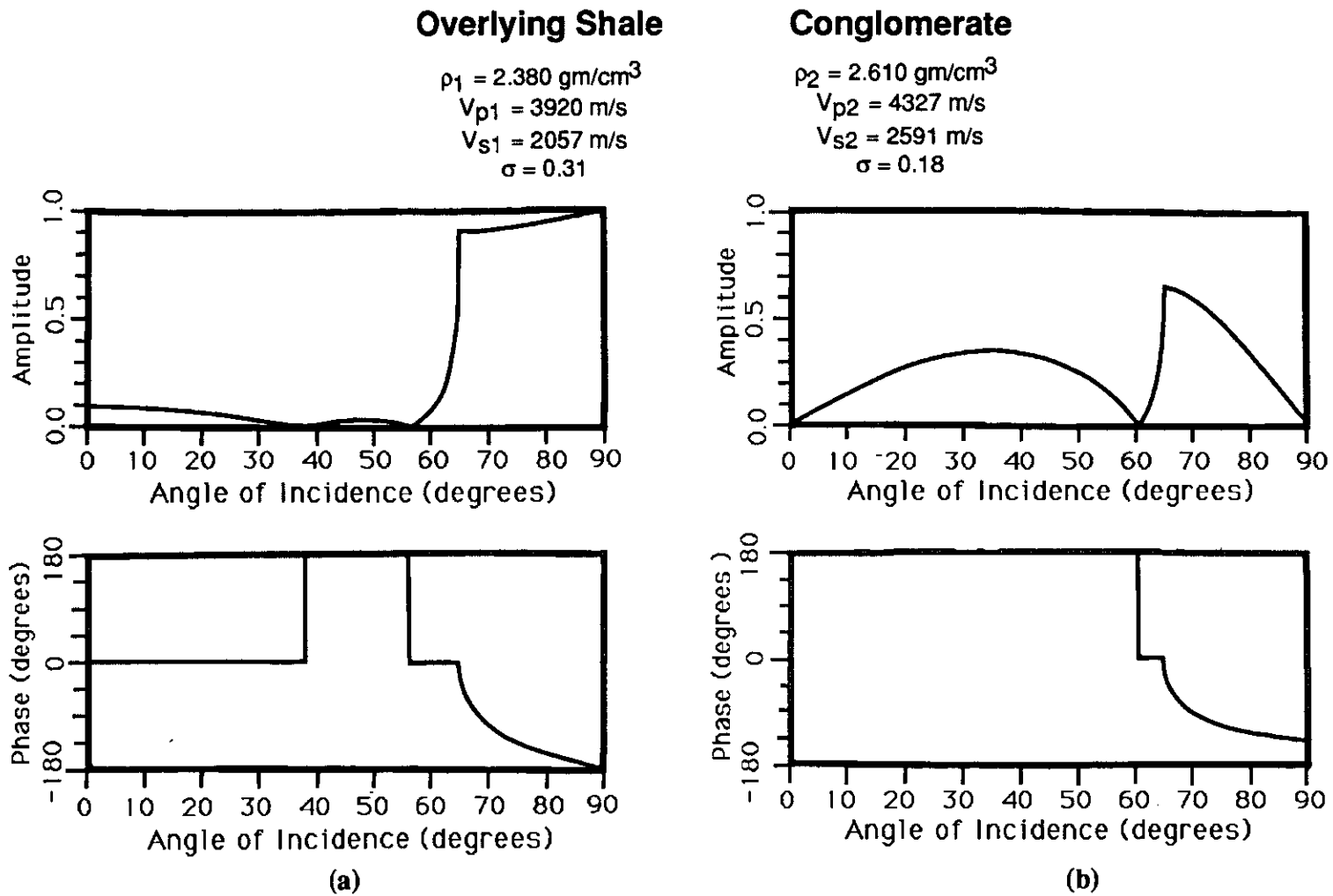


FIG. 10. Amplitude and phase for the (a) P-P and (b) P-SV events from the top of the conglomerate (seismic parameters are listed above). Note the P-P reflection undergoes polarity reversals at  $38^\circ$  and  $56^\circ$  (P-P critical angle occurs at  $65^\circ$ ).

### Conglomerate

$\rho_2 = 2.610 \text{ gm/cm}^3$   
 $V_{p2} = 4327 \text{ m/s}$   
 $V_{s2} = 2591 \text{ m/s}$   
 $\sigma = 0.18$

### Underlying Shale

$\rho_3 = 2.510 \text{ gm/cm}^3$   
 $V_{p3} = 4003 \text{ m/s}$   
 $V_{s3} = 2100 \text{ m/s}$   
 $\sigma = 0.31$

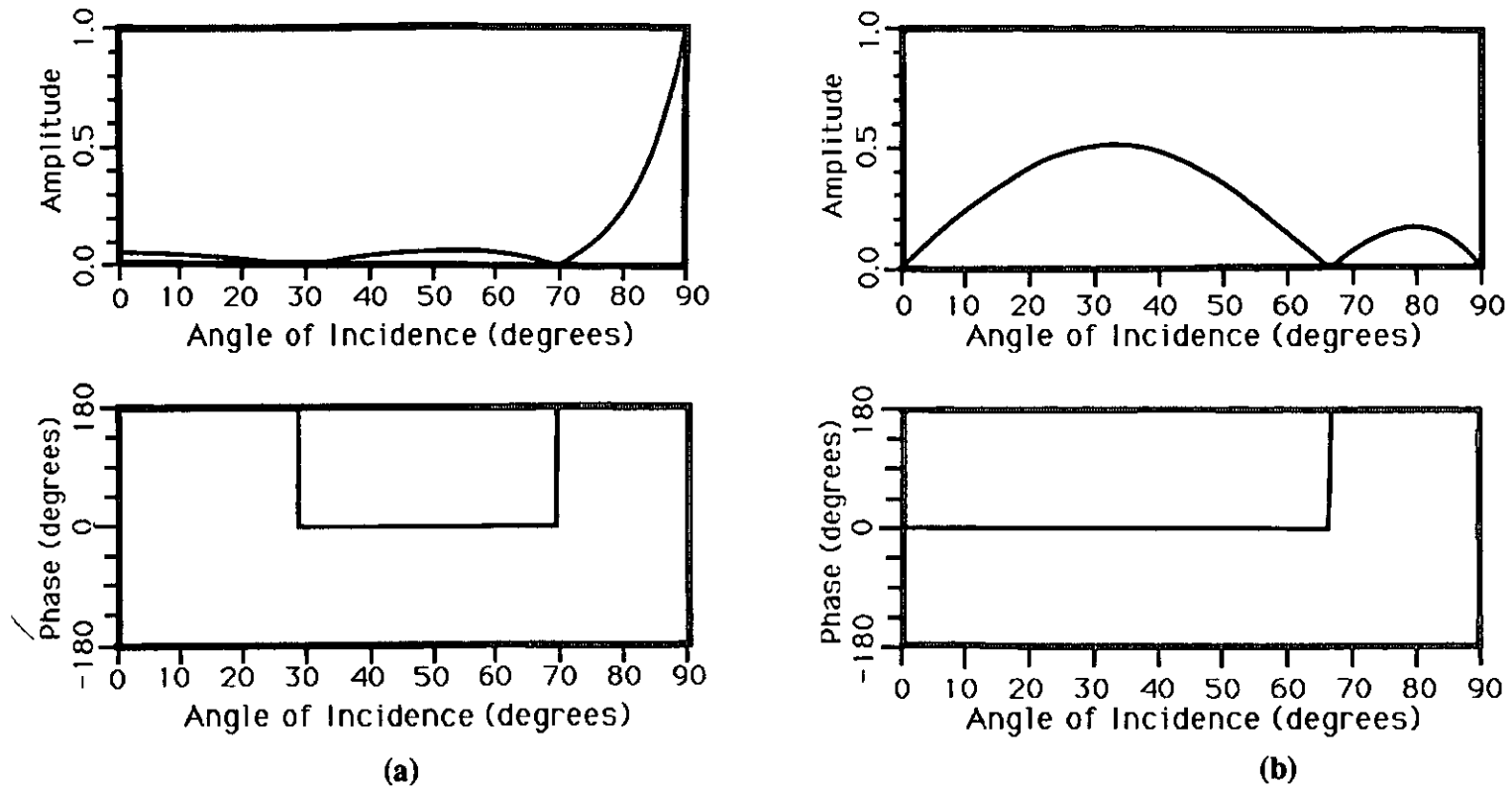


FIG. 11. Amplitude and phase for the (a) P-P and (b) P-SV events from the bottom of the conglomerate (seismic parameters are listed above). Note the P-P polarity reversals at 29° and 70° (no P-P critical angle is present).

the events) has to be determined. Figure 12 shows an example of the seismic response with respect to offset (ie. the AVO response) of the P-P and P-SV reflections for the top, bottom, and combined interfaces of a 15 m-thick conglomerate having a Poisson's Ratio of 0.22. The combined response will hereafter be referred to in this study as the Cardium event. Note the polarity reversal that occurs with offset in the combined response for the P-P but not the P-SV Cardium event. The P-P peak-trough response at near-offsets becomes a trough-peak at far-offsets, whereas the P-SV trough-peak response occurs over all offsets. Another feature of the P-P data is an amplitude minimum at mid-offsets while a corresponding maximum is observed in the P-SV case.

To gain a full understanding of the conglomerate AVO response, the effect of variation in the conglomerate's Poisson's Ratio and thickness had to be modeled.

### **Thickness dependency**

Figure 13 shows the P-PAVO response and corresponding amplitude of the Cardium peak, for conglomerate thicknesses ranging from 5 to 20 m. This figure shows the P-P data to be highly sensitive to variation in conglomerate thickness, with the sensitivity being greatest in the near-offset range (0-1000 m). As mentioned previously, an amplitude minimum is observed in the mid-offset range (1000-2000 m). Unlike the near- and far-offset ranges, the mid-offset range exhibits an amplitude decrease with increasing conglomerate thickness.

The P-SV AVO response and corresponding amplitudes of the Cardium trough are shown in Figure 14 for the same range of thicknesses as in Figure 13. The P-SV data also shows a strong sensitivity to variation in conglomerate thickness. In this case, however, the greatest sensitivity is observed in the mid-offset range (1000-2000 m) with increasing thickness causing increasing amplitudes.

### **Poisson's ratio dependency**

Figure 15 shows the P-P AVO response and corresponding amplitudes of the Cardium peak for Poisson's Ratios of the conglomerate varying from 0.15 to 0.28. All variations in Poisson's Ratio were obtained by changing  $V_s$  and keeping  $V_p$  constant. As in the case for variation in thickness (Figure 13), this figure also shows the P-P data to be highly sensitive to variation in Poisson's Ratio. In this case, however, the greatest sensitivity is observed in the far-offset range (>1500 m). Increasing Poisson's Ratio, in effect, shifts the amplitude minimum from the mid-offsets to the far-offsets. However, this far-offset dependency upon Poisson's Ratio would most likely not be observed on the vertical component Carrot Creek data since the majority of the far-offset data have been removed by the front-end mute.

Unlike the case of varying the conglomerate thickness, Figure 16 shows that the P-SV AVO response of the conglomerate is not nearly as sensitive to variation in Poisson's Ratio. Much smaller increases in amplitude are observed in the mid-offset range (1000-2000 m), for decreasing Poisson's Ratio, than is observed when the thickness of the conglomerate is increased (Figure 14).



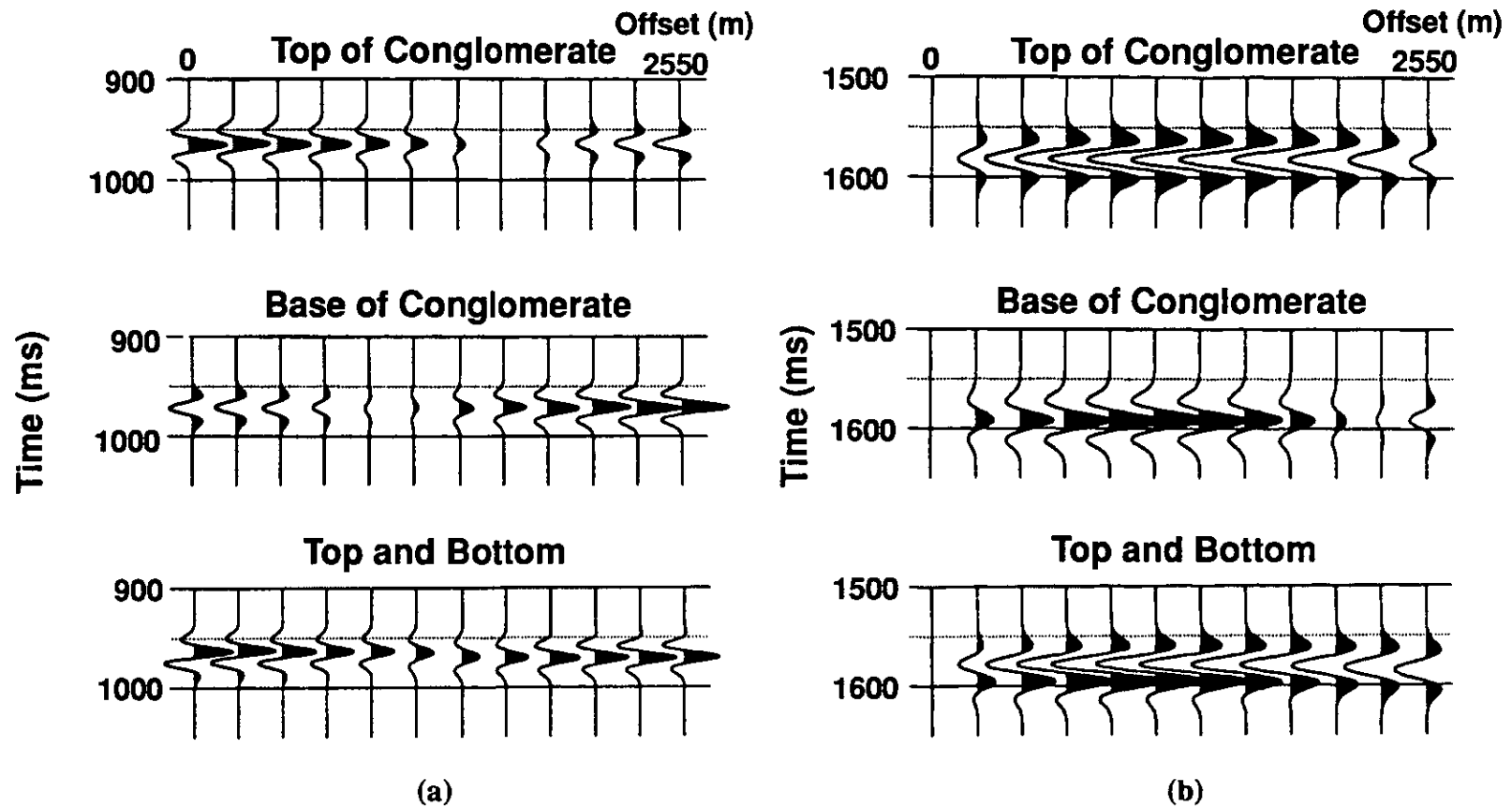
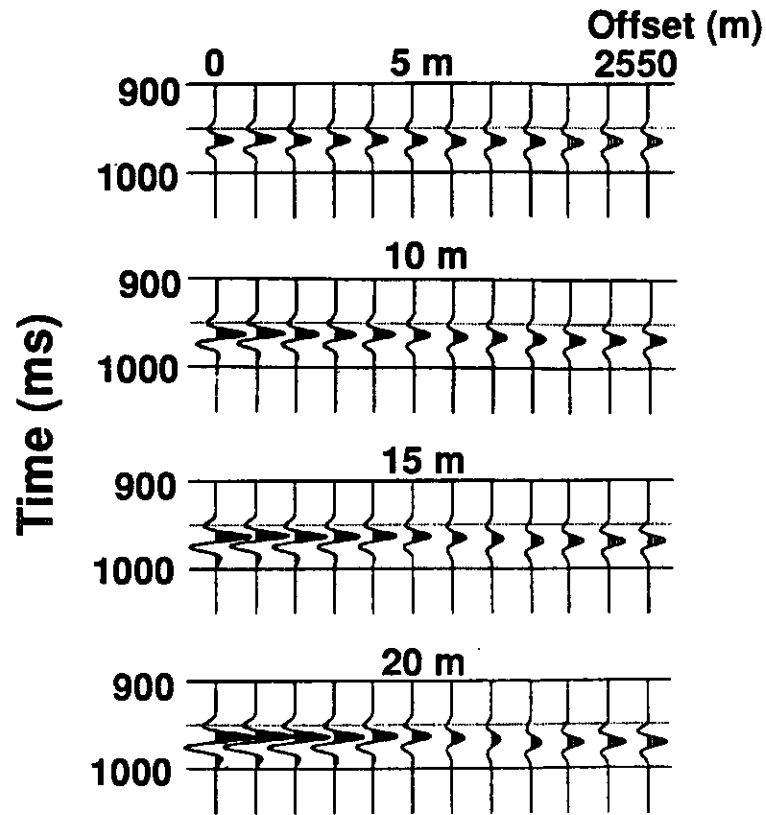
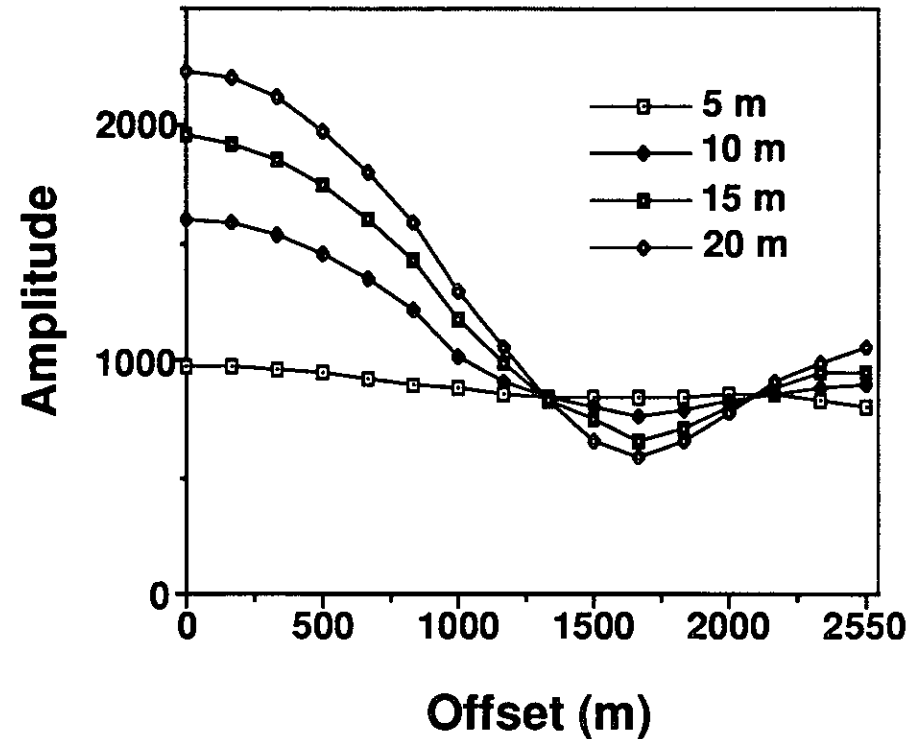


FIG. 12. Cardium AVO response for (a) P-P and (b) P-SV case of a 15 m thick conglomerate with a Poisson's Ratio of 0.22. The Poisson's Ratio of the over- and underlying shales is kept at 0.31. Note that a polarity reversal occurs with the combined P-P event but not the P-SV event.



(a)



(b)

FIG. 13. The effect of variation in conglomerate thickness on the P-P (a) seismic response and (b) the amplitude of the Cardium peak. The Poisson's Ratio of the conglomerate and the over- and underlying shales are kept at 0.22 and 0.31 respectively. Note the Cardium Peak amplitude is at a minimum at mid-offsets and shows greatest sensitivity to thickness variations at near-offsets.

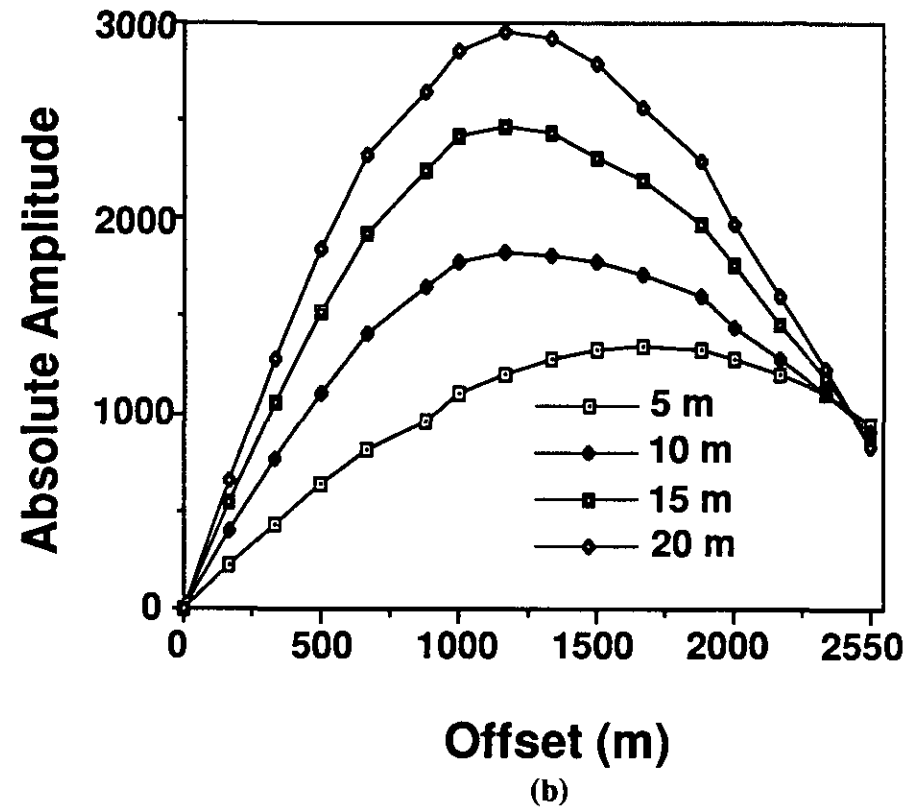
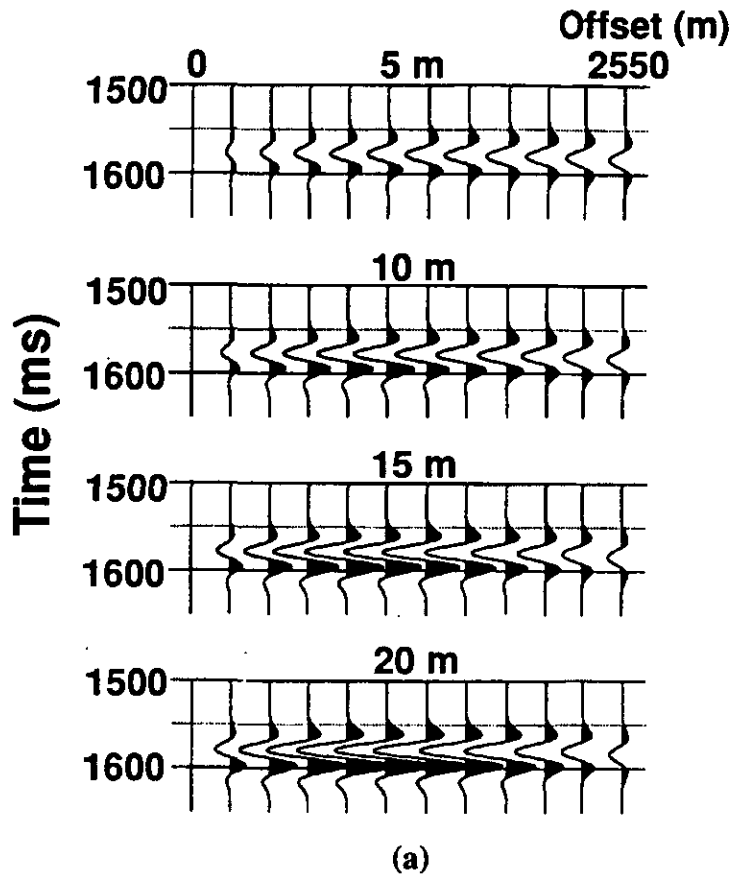


FIG. 14. The effect of variation in conglomerate thickness on the P-SV (a) seismic response and (b) the amplitude of the Cardium trough. The Poisson's Ratio of the conglomerate and the over- and underlying shales are kept at 0.22 and 0.31 respectively. Note the amplitude of the Cardium trough shows the greatest sensitivity at thickness variations at mid-offsets.

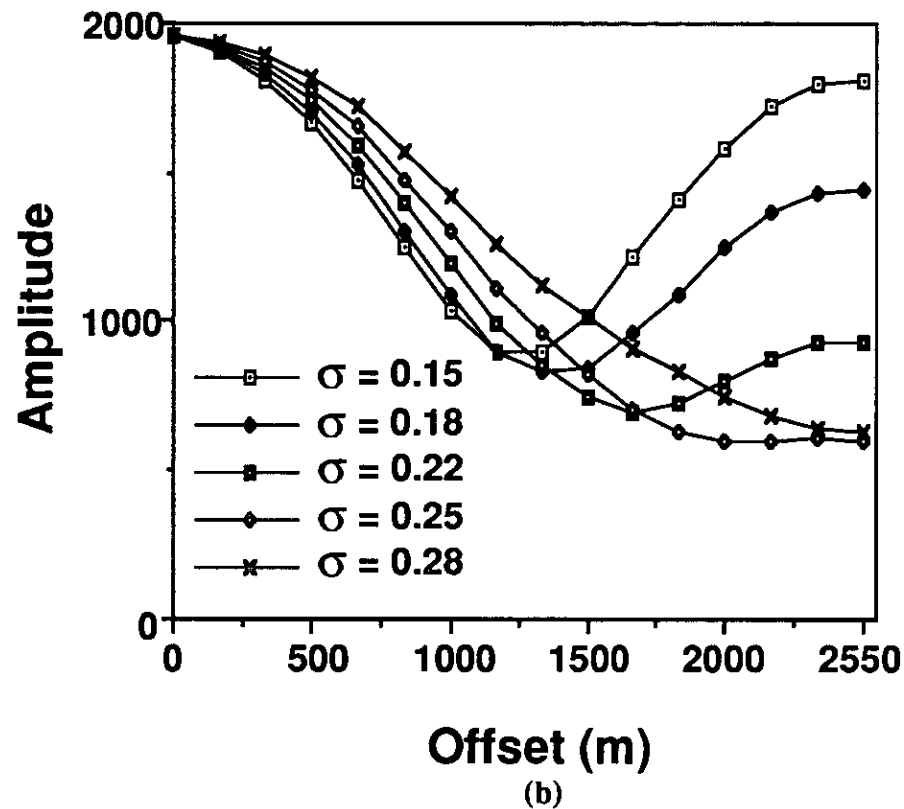
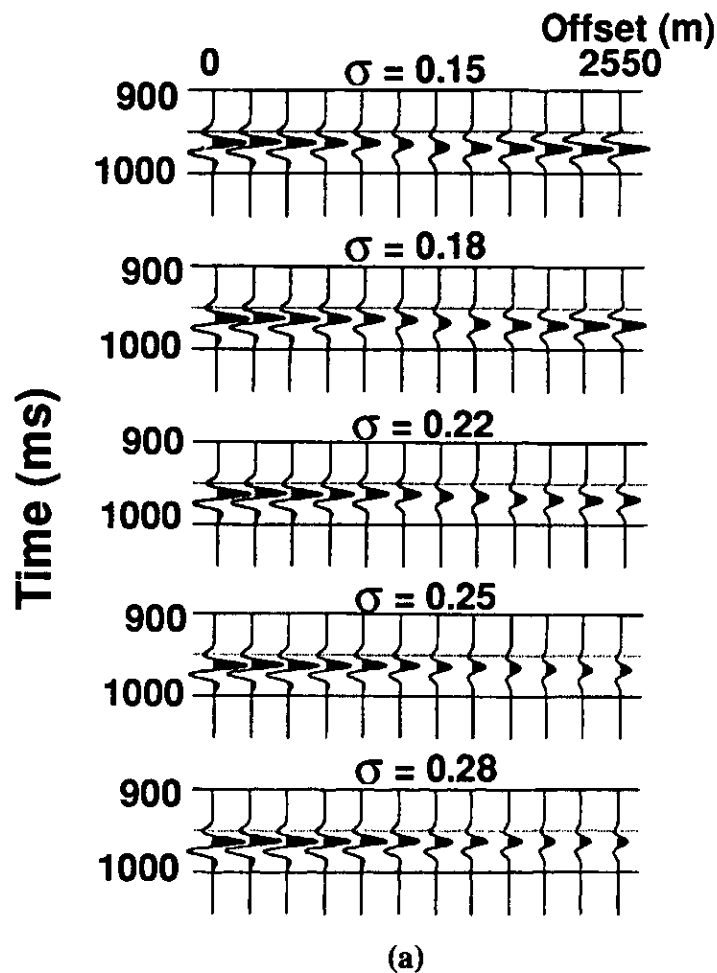


FIG. 15. The effect of variation in the conglomerate's Poisson's Ratio on the P-P (a) seismic response and (b) the amplitude of the Cardium peak. The conglomerate's thickness and the Poisson's Ratio of the over- and underlying shales are kept at 15 m and 0.31 respectively. Note the amplitude of the Cardium peak exhibits the greatest sensitivity to variation in Poisson's Ratio at far-offsets

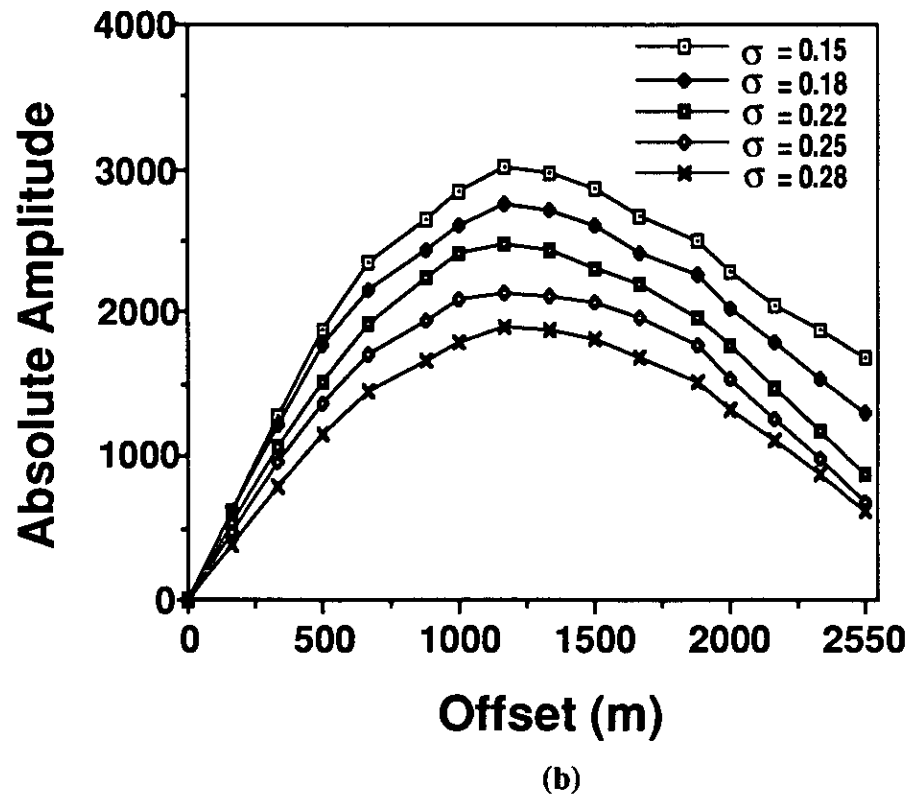
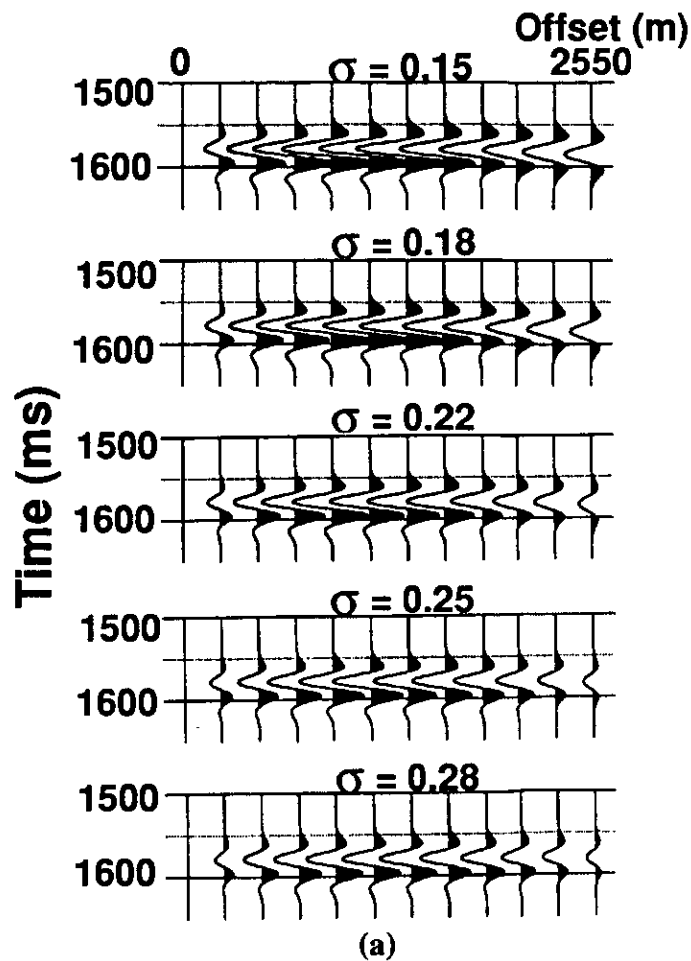


FIG. 16. The effect of variation in the conglomerate's Poisson's Ratio on the P-SV (a) seismic response and (b) the amplitude of the Cardium trough. The conglomerate's thickness and the Poisson's Ratio of the over- and underlying shales are kept at 15 m and 0.31 respectively. Note the amplitude of the Cardium trough is does not show great sensitivity to variation in Poisson's Ratio.

## AVO ANALYSIS OF REAL DATA

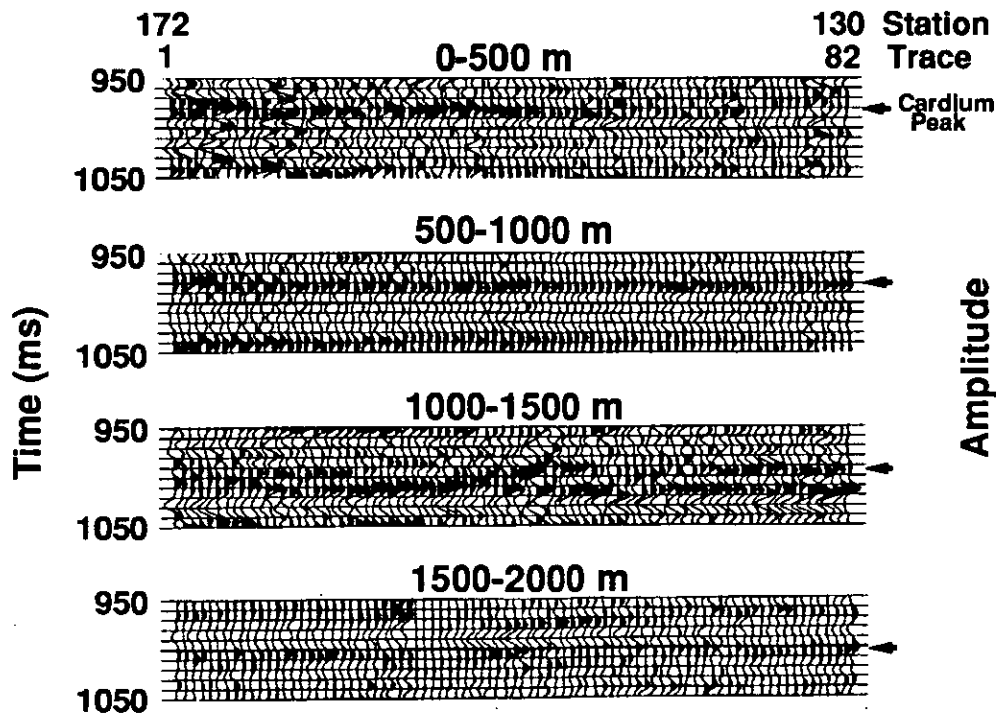
In order to see if any of these AVO effects are present in the surface seismic data, various offset-range stacks were produced from the vertical (P-P) and radial (P-SV) components of the multicomponent seismic lines. The offset-stacks were generated over 500 m intervals (ie. 0 - 500 m, 500 - 1000 m, etc.). For both the P-P and P-SV cases, the 2000 - 2500 m stacks were not generated since the Cardium event in this range was partially removed by the front-end mute. Figure 17 and 18 show the offset-stacks of a portion of the vertical- and radial-component stacks of lines CCSW02 and their respective amplitudes for the Cardium event (ie. peak for the vertical-component and trough for the radial-component). These portions of the seismic line were chosen because of their high signal-to-noise ratio. To help reduce random noise for the picking of the amplitudes, a trace mix (weighting: 10-20-40-20-10) was applied over 5 adjacent traces.

The results from both the P-P (vertical-component) and P-SV (radial-component) offset-stacks support the conclusions predicted by modeling. The P-P case, for instance, shows a change in character from a Cardium peak-trough at near-offsets to a trough-peak at far-offset due to a polarity reversal (indicated by the downward shift in the Cardium peak with increasing offset). Amplitudes of the various stacks also indicate a minimum at mid-offset ranges on the vertical-component. An interesting feature of these stacks is that although the 0-500 m offset-range generally possesses higher amplitudes than the 500-1000 m range, the Cardium event appears to be more coherent in the 500-1000 m range. This phenomenon was also documented by Wren (1984) and appears to arise because of the presence of source-generated air-waves in the 0-500 m offset-range. This results in a greater fluctuation in the Cardium amplitude which in turn causes a decrease in coherency after scaling of the data. The P-SV case, on the other hand, shows the greatest amplitude in the mid-offset ranges (500-1000 m, 1000-1500 m and 1500-2000 m). The 0-500 m offset-range exhibits significantly lower amplitudes due to less P-SV conversion occurring.

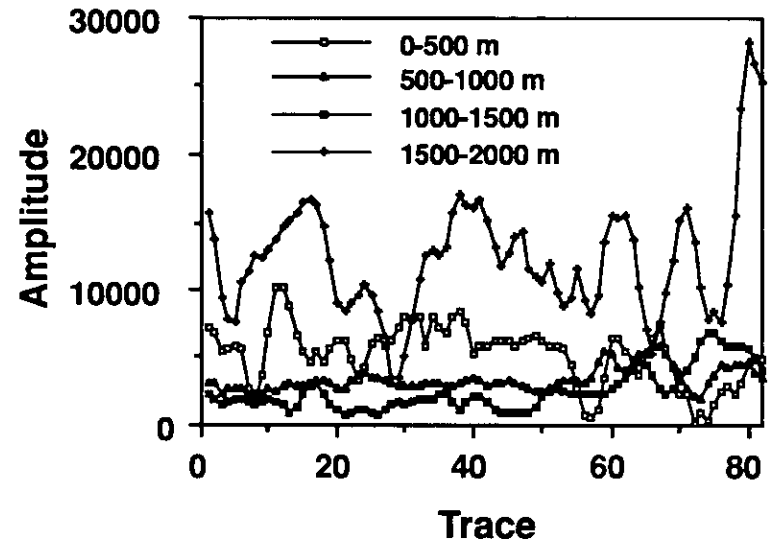
## LATERAL CHANGES IN $V_p/V_s$

As demonstrated previously,  $V_p/V_s$  information can be extracted from multicomponent seismic data using vertical- and radial-component isochron values. Instead, however, of using this technique to obtain  $V_p/V_s$  values at one location, as done previously, values can be calculated along the entire seismic line, and using equation 2, Poisson's Ratio profiles can be generated. These profiles, in turn, can be used to identify lateral variations in Poisson's Ratio, which may be indicative of lithologic changes within a specific interval.

This Poisson's Ratio interval analysis was found to be useful in identifying variation in the thickness of the Cardium conglomerate in the Carrot Creek field. This ability arises from the conglomerate having a high P-wave velocity and a low  $V_p/V_s$  value relative to the surrounding shales. Because of the higher velocity of the conglomerate, variation in conglomerate thickness will produce varying amounts of pull-up of underlying events. This pull-up will in turn decrease the isochron of any interval in which the conglomerate is contained. The thicker the conglomerate, the larger the pull-up of underlying events and therefore the greater the thinning of the isochron. Because of the low  $V_p/V_s$  of the conglomerate, a larger relative velocity contrast will occur between the conglomerate and the surrounding shales for S- than P-waves (ie. the average difference between the conglomerate and the surrounding shales for the S- and P-wave velocities are 25% and 9% respectively). This difference in velocity contrasts will therefore result in a greater amount of isochron

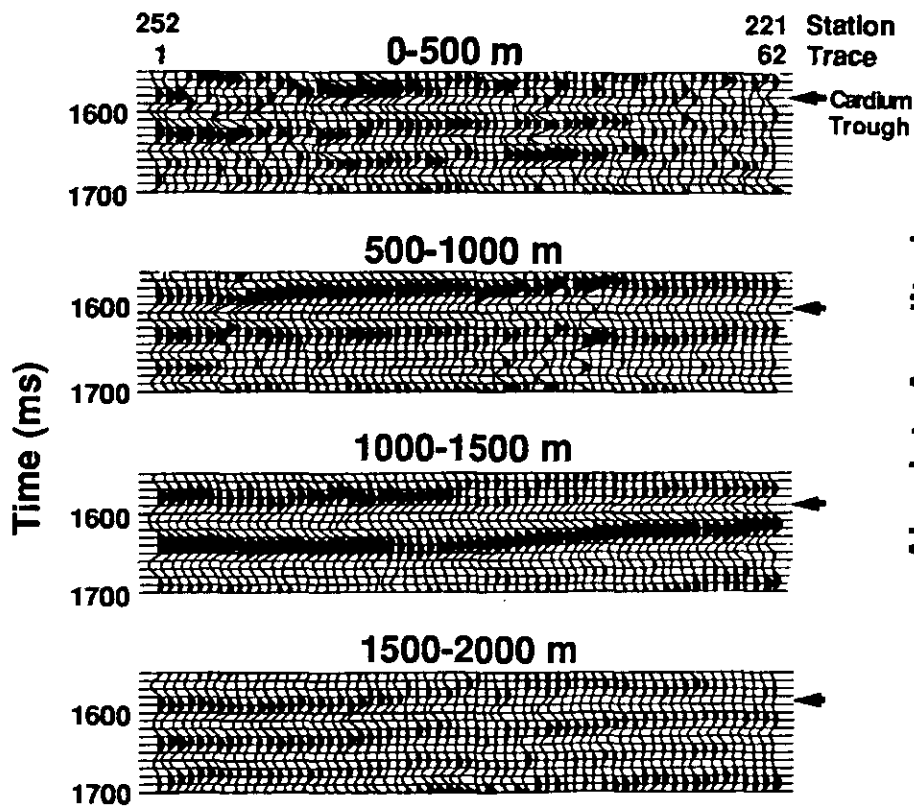


(a)

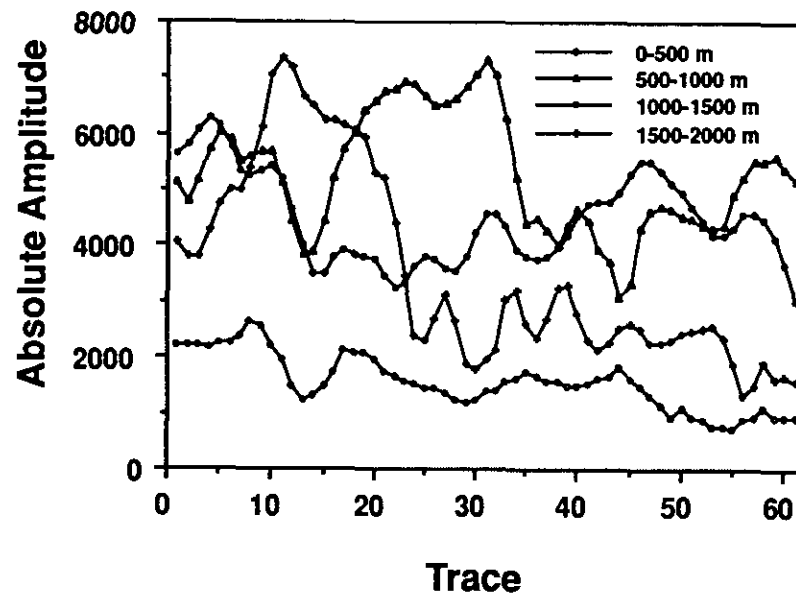


(b)

FIG. 17. (a) Offset-stacks of the P-P (vertical-component) data of line CCSW02 and the (b) amplitudes of the corresponding Cardium peaks. Note how the Cardium peak becomes delayed in panels of greater offset and exhibits an amplitude minimum at mid-offsets.



(a)



(b)

FIG. 18. (a) Offset-stacks of the P-SV (radial-component) data of line CCSW02 and the (b) amplitudes of the corresponding Cardium troughs. Note how the amplitude of the Cardium trough exhibits a maximum at mid-offsets.



thinning for P-SV than P-P data as the conglomerate thickness increases. Using equation 1 and 2, this discrepancy in isochron thinning will then result in  $V_p/V_s$ , and therefore Poisson's Ratio, lows in areas of thick conglomerate.

In this thesis, the Poisson's Ratio analysis was undertaken over three intervals; Lea Park - Blackstone, Lea Park - Base of Blackstone and Lea Park - Second White Specks. These intervals were chosen because they can be confidently correlated between the vertical- and radial-component seismic sections, in addition to containing the Cardium conglomerate. The close proximity of these events to the conglomerate is also important, because the smaller the isochron interval the greater the effect the conglomerate will have upon the interval  $V_p/V_s$  and therefore the Poisson's Ratio deduced.

The results of this analysis for line CCSW01 are shown in Figure 19. Two Poisson's Ratio lows are observed on these profiles, indicating that, as the seismic interval increases (ie. Lea Park - Second White Specks to Lea Park - Blackstone), the lows in the Poisson's Ratio become less apparent. The attenuation of these lows with increasing interval size arise because the conglomerate contributes less to the overall velocity of the interval.

Due to the lower signal-to-noise ratio of line CCSW02, the coherency of the events was not as strong as CCSW01 and therefore the same analysis could not be undertaken with any confidence.

## DISCUSSION

### Event amplitude

As indicated by Figure 7 most of the major P-P (vertical-component) reflections correlate well with P-SV (radial-component) reflections, with only differences in relative amplitude between events being present. The most significant differences in amplitude occurs with the Viking and Cardium events. Figures 8 and 9 show, for instance, that the Viking event exhibits anomalously high amplitudes relative to the other P-SV events, compared to the P-P data. These large Viking amplitudes are surprising since the angles of incidence on this interface are less than 10 degrees (ie. little P-SV conversion should be occurring). These large amplitudes are in fact due to tuning of three events; the Viking, the Joli Fou and the Mannville.

The Cardium event, on the other hand, exhibits two strong amplitude anomalies on both of the P-SV sections while only a very subtle amplitude increase can be observed on the P-P sections at these same locations (Figure 20). This significant difference in amplitude between the P-P and P-SV data can be attributed to the AVO effect modeled earlier. More specifically, the weaker P-P amplitudes arise because of a polarity reversal observed with increasing offset. Therefore, upon stacking the Cardium P-P event will become attenuated due to destructive interference as the near- and far-offset are stacked together. The event of the radial component, on the other hand, does not exhibit a polarity reversal and therefore traces over all offsets will stack constructively, producing a much stronger Cardium response.

Because the P-SV response is much more sensitive to variation in conglomerate thickness than Poisson's Ratio, the P-SV amplitude anomalies are interpreted to be caused by an increase in conglomerate thickness. This is supported by the fact that these anomalies

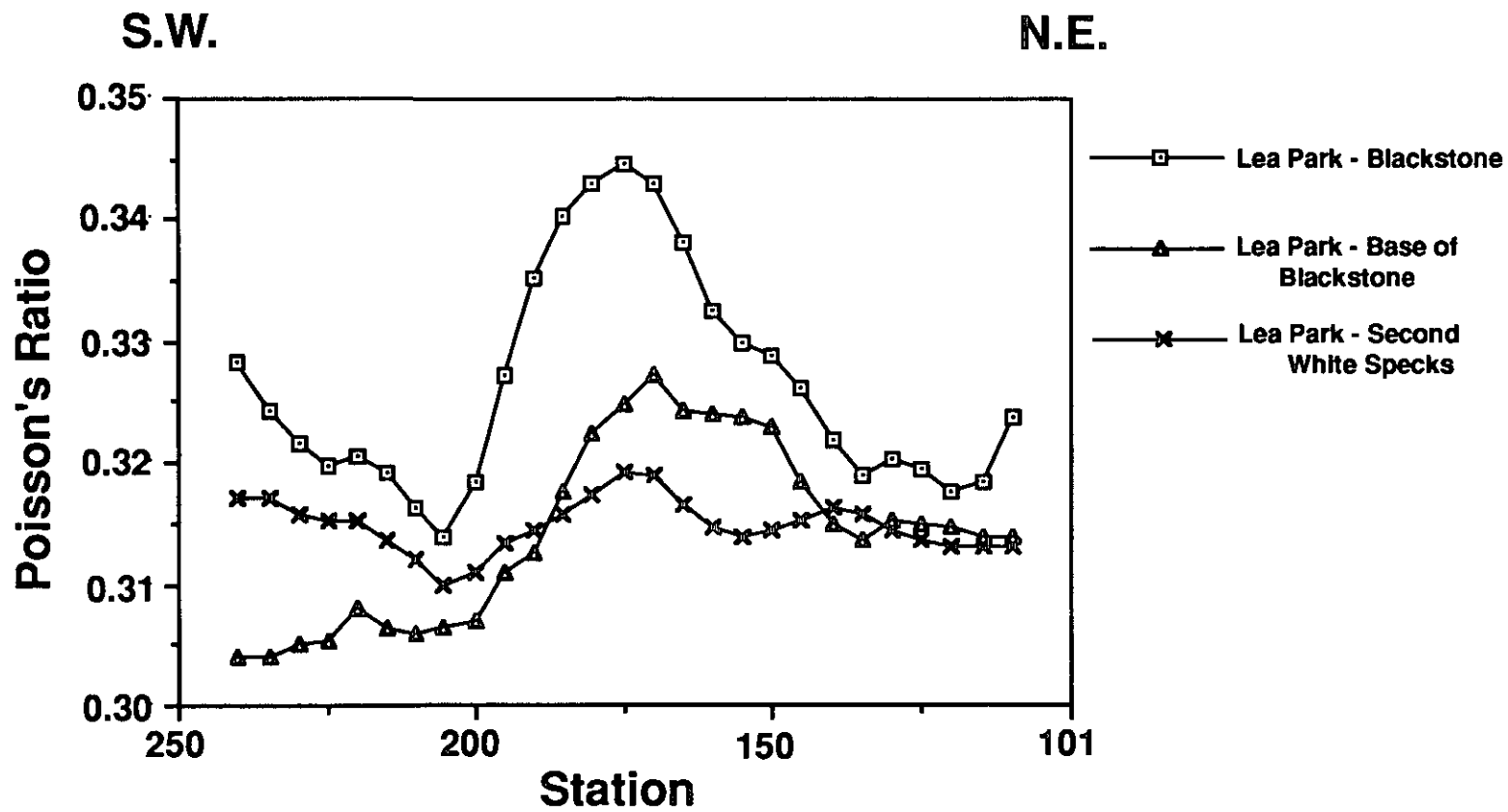


FIG. 19. Interval Poisson's Ratios calculated from line CCSW01 using various isochrons (isochrons listed above). Note the lows in Poisson's Ratio towards the ends of the line, due to the presence of thick conglomerates.

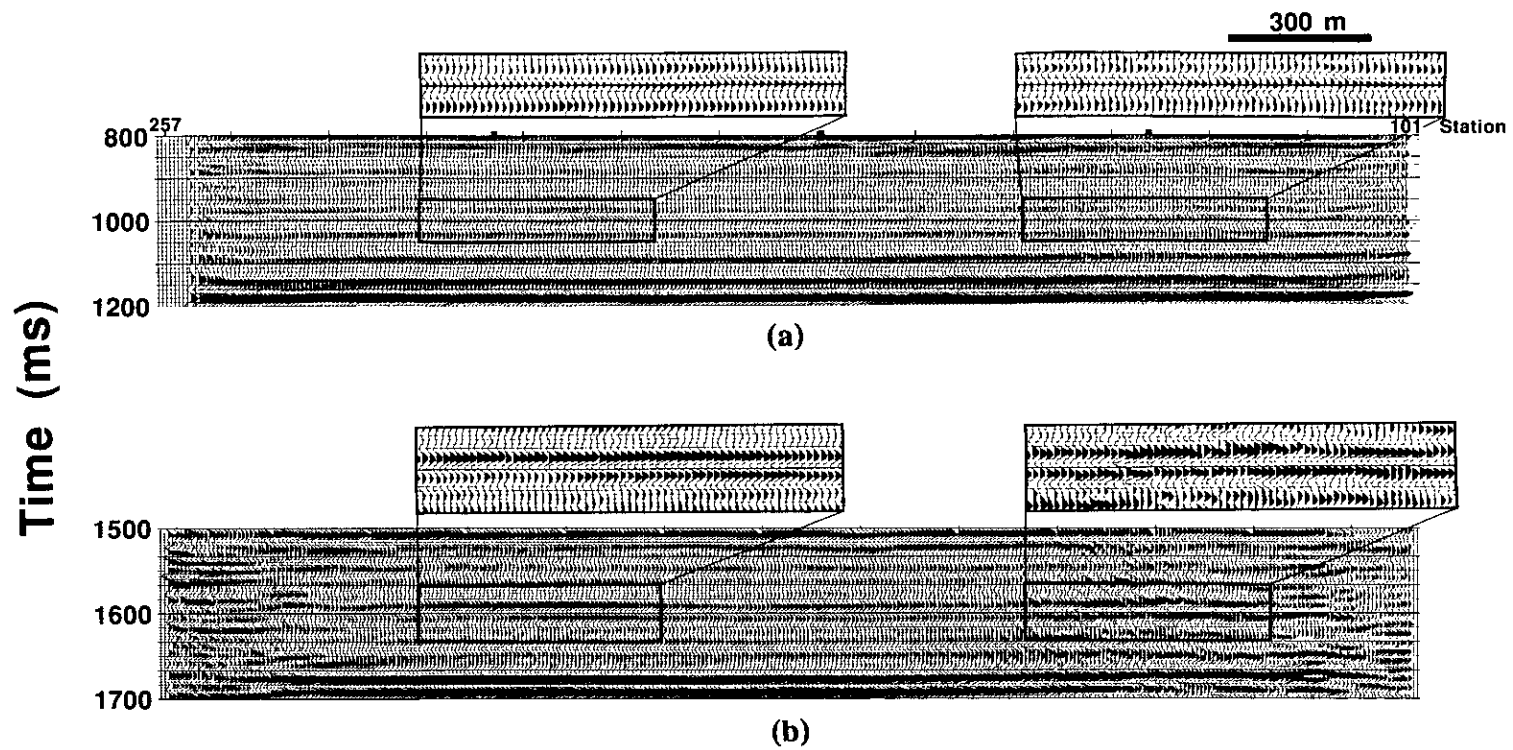


FIG. 20. Cardium event of the (a) vertical- and (b) radial-components of line CCSW01 with the amplitude anomalies highlighted.

occur at the location of presently producing, thick conglomerate bodies. This is also supported by Figure 21 which shows the correlation between the P-SV amplitude anomalies with increases in the conglomerate isopach and lows in the calculated Poisson's Ratios (Lea Park - Blackstone interval); ie. both indicating an increased conglomerate thickness.

### **Offset-range stacking**

From the AVO modeling, it can also be concluded that full-offset stacking, can be detrimental for the P-P reflection, when large source-receiver offsets are acquired. Figure 13 indicates that the vertical-component should in fact better resolve the conglomerate and variation in its thickness, using a near-offset stack. This figure shows that the P-P near-offsets should exhibit large amplitudes that should be highly sensitive to the thickness of the conglomerate (ie. assuming the conglomerate has a low Poisson's Ratio). This is contrary to the P-SV data which shows its greatest sensitivity to conglomerate thickness at mid-offsets 14. Figure 22 shows the P-P Cardium event of line CCSW01 from a 0-1000 m offset-stack, along with the corresponding P-SV Cardium event. As predicted, significantly stronger P-P amplitude anomalies, than observed in the full-offset stack of Figure 20, can now be seen at the same location as the P-SV anomalies. This, in turn, helps support the conclusion that the P-SV anomalies are indeed due to the presence of thicker conglomerates.

### **Limiting the far-offset**

It has generally been believed that, when acquiring multicomponent seismic data, large source-receiver offsets are desirable. The results discussed above, however, indicate that in the Carrot Creek field this is not necessarily the case. The far-offsets of the Carrot Creek field, for example, can be detrimental to the imaging of the P-P Cardium event when generating full-offset stacks. In addition, as indicated by the AVO modeling results and the amplitude plots of Figures 10 and 11, its the P-SV mid-offsets (500-2000 m) which exhibit the greatest amount of conversion, not the far-offsets (>2000 m). It can therefore be concluded that larger offsets are not necessarily always better in the acquisition of multicomponent data. Better imaging can often be obtained by either limiting the offset-range during acquisition or by generating offset-range stacks.

## **CONCLUSIONS**

The acquisition of multicomponent seismic data not only records conventional P-wave data but also S-wave data. This S-wave data, in turn, can provide additional information concerning the geology of an area. This thesis showed that the recording of P-SV data can in fact help delineate geologic units, particularly the Cardium conglomerates of the Carrot Creek field. The Carrot Creek multicomponent data, for instance, exhibits only subtle amplitude variations, on the vertical (P-P) component, whereas at the location of conglomerate bodies, strong amplitude anomalies can be observed on the radial (P-SV) component. Through the analysis of the P-P and P-SV seismic responses several additional conclusions concerning the Carrot Creek multicomponent data set can be made.

- 1) Differences in amplitude of the Cardium event between the P-P and P-SV final stacks is a result of the difference in their respective AVO responses. AVO forward modeling showed that a polarity reversal occurs with offset for the P-P but not the P-

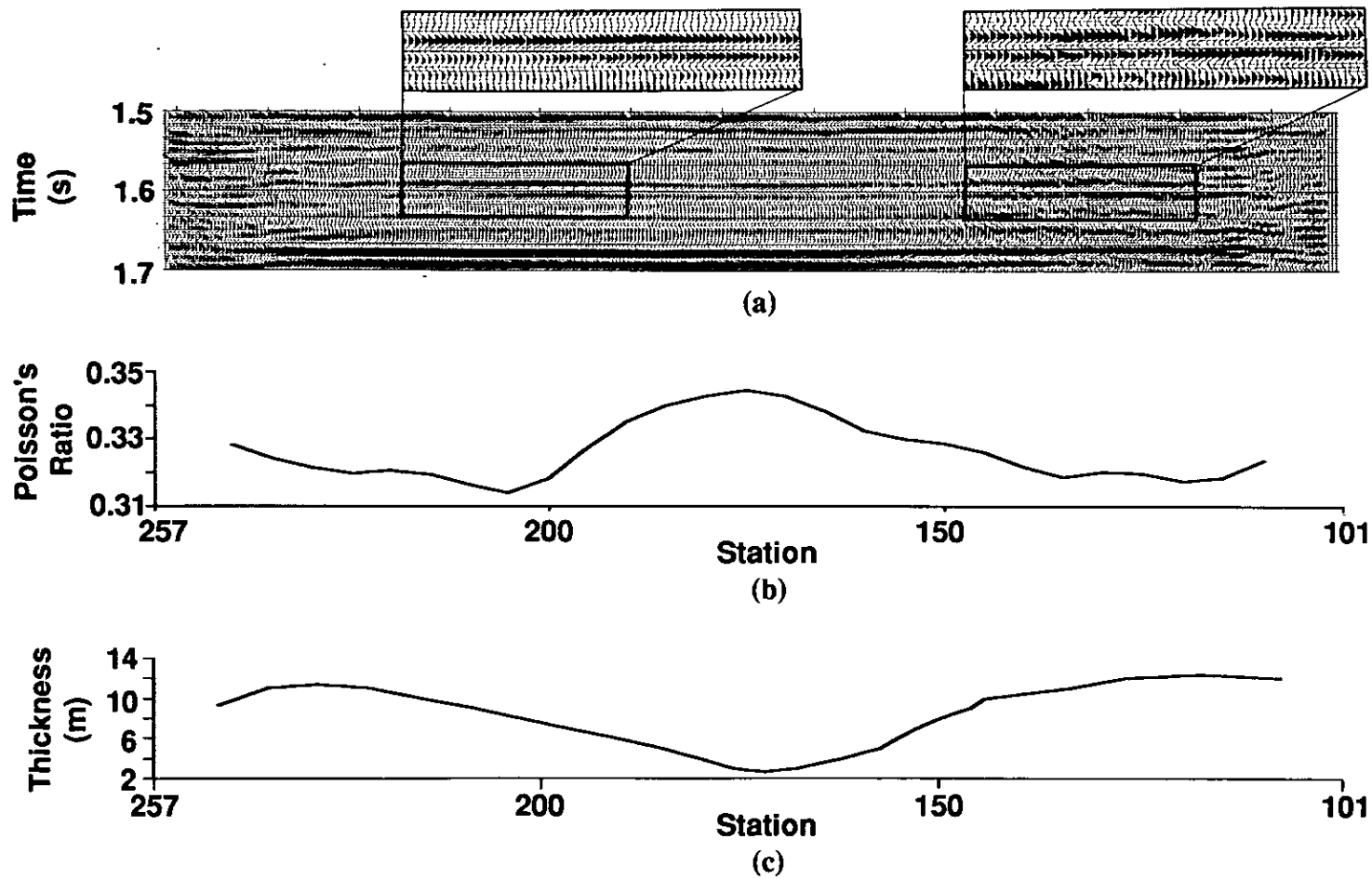


FIG. 21. Comparison of (a) the P-SV anomalies, (b) the Poisson's Ratio calculated for the Lea Park - Blackstone interval and (c) the thickness of the conglomerate interval

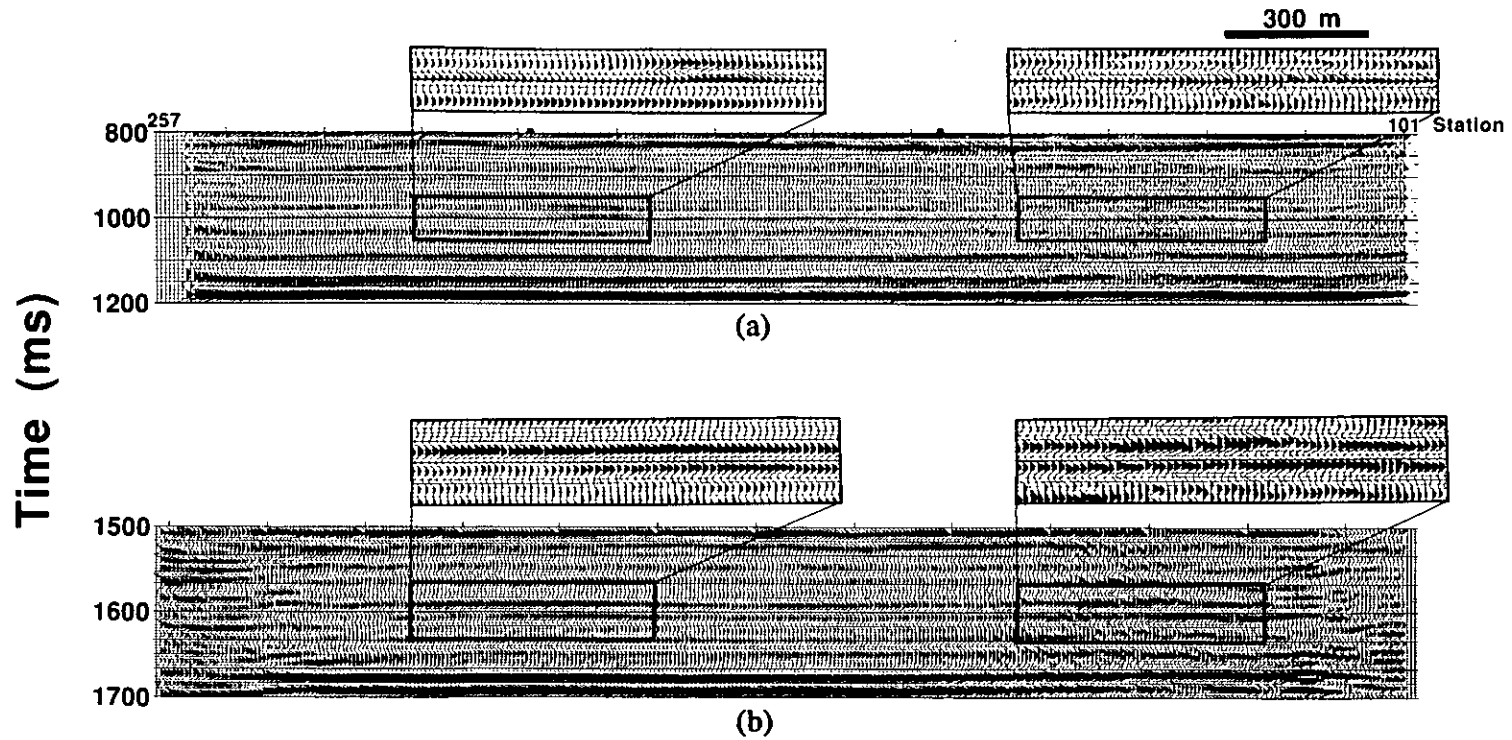


FIG. 22. Comparison of the Cardium event from (a) a 0-1000 m P-P offset-range stack and (b) the final radial-component stack of line CCSW01. A strong P-P Cardium amplitude anomaly occurs at the same location as the P-SV amplitude anomalies.

SV case. It is this polarity reversal which causes the attenuation of the P-P Cardium event relative to the P-SV event. Upon stacking the near- and far-offsets of the P-P data add destructively, whereas the radial component offsets add constructively producing in a much stronger P-SV Cardium event.

2) Due to their respective AVO responses the P-P and P-SV data are most sensitive to the thickness of the Cardium conglomerate over different offset-ranges. The P-P data, for instance, exhibits the greatest sensitivity in the first 1000 m of offset (ie. before the polarity reversal). The radial component, on the other hand, is most sensitive over the 500-2000 m offset-range.

3) Using both P-P and P-SV data, estimates for Poisson's Ratio for specific seismic intervals can be calculated. Since the Cardium conglomerate possesses a low Poisson's Ratio (0.18-0.22), relative to the surrounding shales (0.31), this interval analysis was capable of identifying variations in conglomerate thickness by the presence of lows in the calculated Poisson's Ratio. Two such lows could be identified on line CCSW01 which correlate well with the location of thick conglomerates.

4) Better imaging of the Cardium conglomerate can be achieved by either limiting the offset-range during acquisition or by generating offset-range stacks. For example, as shown in this study, limiting the P-P data to the 0-1000 m offset-range results in the ability to identify locations of thick Cardium conglomerate deposits: ie. no destructive interference occurs as in the case when all offsets are stacked together. The P-SV data, on the other hand, was limited to the first 2000 m offset by the thickness sensitivity, mentioned above, and by the presence of refracted energy present in the 2000-2500 m offset-range.

In conclusion the use of multicomponent seismic data appears to show excellent promise in hydrocarbon exploration. Not only does it give an independent estimate of the subsurface geologic structure, but also may give an indication of variations in lithologies.

## ACKNOWLEDGEMENTS

We would like to thank Boyd Exploration for the donation of the multicomponent and Dr. Ed Krebs (University of Calgary) for the generation of the amplitude and phase plots. We would also like to thank the sponsors of the CREWES Project for their continued support.

## REFERENCES

- Bergman, K.M. and Walker, F.G., 1987, The importance of sea-level fluctuations in the formation of linear conglomerate bodies: Carrot Creek Member of the Cardium Formation, Cretaceous Western Interior Seaway, Alberta, Canada: *Journal of Sedimentary Petrology*, **57**, 651-665.
- Harrison, M., 1989, Three-component seismic data processing: Carrot Creek Alberta: CREWES Project Research Report, Volume 1, 6-26.
- Howell, C.E., Lawton, D.C., Krebs, E.S., and Thurston, J.B., 1991, P-SV and P-P synthetic stacks: this volume.
- Joiner, S., 1989, Sedimentology and ichnology of the Cardium Carrot Creek field, West Central Alberta, Course work: Geology 701, University of Calgary.
- Krause, F.F. and Nelson, D.A., 1984, Storm event sedimentation: lithofacies formation in the Cardium Formation, Pembina area, West Central Alberta, Canada: in Stoth, D.F. and Glass, D.J. eds., *The Mesozoic of Middle North America*, C.S.P.G. Memoir 9, 485-511.

- Plint, A.G., Walker, R.G. and Bergman, K., 1986, Cardium Formation 6: Stratigraphic framework of the Cardium in the subsurface: *Bulletin of Canadian Petroleum Geology*, **34**, 213-225.
- Williams, G.D. and Burk, C.F. Jr., 1964, Upper Cretaceous: in McCrosson, R.G. and Gallister, R.P. eds., *Geological History of Western Canada*, A.S.P.G., Calgary, Alberta, 169-189.
- Wren, E.A., 1984, Seismic techniques in Cardium exploration: *Journal of the Canadian Society of Exploration Geophysicists*, **20**, 55-59.